ADDIS ABABA UNIVERSITY
SCHOOL OF GRADUATE STUDIES
School of Civil and Environmental Engineering

The Effect of Track Irregularities on Wheel-Rail Contact Relationship

By

Tadios Sisay Habite

A Thesis Submitted to School of Civil and Environmental Engineering in Partial Fulfillment of the Requirement for Degree of

Master of Science

In

Civil Engineering (Railway Engineering)

Advisor
Ato Mequanent Mulugeta (M.Sc.)

July, 2016
Addis Ababa, Ethiopia

ADDIS ABABA UNIVERSITY
SCHOOL OF GRADUATE STUDIES
School of Civil and Environmental Engineering

The Effect of Track Irregularities on Wheel-Rail Contact Relationship

By

Tadios Sisay Habite

A Thesis Submitted to School of Civil and Environmental Engineering in Partial Fulfillment of the Requirement for Degree of

Master of Science

In

Civil Engineering (Railway Engineering)

Approved by Board of Examiners

Ato Mequanent Mulugeta	____________	____________
Advisor	*Signature*	*Date*
Ato Abdulsetar Siraj	____________	____________
Internal Examiner	*Signature*	*Date*
Dr. Esayas G/Youhannes	____________	____________
External Examiner	*Signature*	*Date*
Dr. Birhanu Beshah	____________	____________
Chairman	*Signature*	*Date*

Acknowledgment

It would have been impossible to fulfil this master thesis without the help and support of the kind people around me, to only some of whom it is possible to give grateful mention here.

First and foremost, I would like to thank God. I am also very grateful to my advisors Ato Mequanent Mulugeta and Ato Matias Kabtamu for offering me the outstanding scientific advices and many discerning suggestions on my research. Ato Mequanint has always been very supportive and constantly provided insightful discussions about the research. For his support and encouragement through the rough road to finish this thesis – personally and academically – I would like to express to him my sincere gratitude. I also have to thank Dr. Tatek Fekadu and Ato Matias Kabtamu who have given valuable comments and constructive feedback on my research proposal as well as on the main thesis body.

Finally, a special thanks to my family and friends for providing me with their unequivocal support without which I could not have completed my thesis. Words cannot express how grateful I am to my parents, they always encourages me and their prayers for me was what sustained me this far.

Abstract

Track irregularity is an inevitable problem in any rail network and it is the source of track deterioration and degradation. This becomes evident in railway projects spanning cities. Hence, the effect of track irregularities on wheel-rail contact relationship is studied with the aim to solve the contact geometry and contact pressure problems induced by these track irregularities. In this regard, independent analysis and parametrization of the rail head surface geometry and the wheel thread geometry is conducted first and the wheel and rail contact point is determined, with the help of the predefined simplified coordinate system.

After the identification of the wheel-rail contact point, mathematically, Hertzian contact theory is applied to calculate the contact area. Accordingly, for an applied normal wheel load of 125kN, the contact area was found to be 118.3 mm^2. Finite element models were also used to simulate the lateral and vertical irregularities, with the help of computer software, ABAQUS. Eight finite element models were analyzed for the study: four for lateral irregularity, three for vertical irregularity, and one model for the tracks without irregularity.

When lateral irregularity is applied on the model the contact pressure on the rail was found to be increasing as compared to the model simulating tracks without irregularity, with a maximum increment of 33.34% for +30mm lateral irregularity. However, contact area and normal contact force induced on the rail decreases by 15.47%, for -8mm and +10mm lateral irregularity, and 15.17%, for +20mm lateral irregularity, respectively.

Similarly, for the applied +30mm vertical irregularity the contact pressure increases by 54.14%, however for +10mm vertical irregularity the contact pressure decreases by 9.15%. Moreover, the +30mm vertical irregularity gives the maximum contact area with a magnitude of 67.66 mm^2.

Keywords – (lateral and vertical) *Track irregularity, Finite element modeling, Hertz contact theory, Parametrization.*

Table of Content

3. ANALYSIS OF WHEEL-RAIL SURFACE GEOMETRY

4. DETERMINATION OF CONTACT AREA

5. FINITE ELEMENT MODELING AND SIMULATION

6. RESULTS AND DISCUSSION

7. CONCLUSION AND RECOMMENDATION

List of Tables

List of Figures

Nomenclatures

A	The ratio of the semi-axes
a	Semi axis in the x direction.
b	Semi axis in the y direction
a_h & b_h	Parameters that depend on the contact geometry and on the material properties of the two contacting surfaces,
$C_{rR}{}^{P}$	Local position vector defining the location of the contact point P with resp the profile coordinate system
D1	Wavelength between 3-25 m
D2	Wavelength between 25-70m
D3	Wavelength between 70-150m
E	Modulus of elasticity
E_r & E_w	Young's modules for the rail and wheel respectively.
e & n	Semi axis coefficients
F_n	The normal contact force applied on the rail
f(y)	The rail profile curve equation
FEM	Finite element modeling
G	The shear modulus
n_{rR}	The normal unit vector
P(x,y)	The ellipsoidal contact pressure distribution
Po	The maximum pressure
P(y)	Parametrized equation of the rail profile curve
Rwx & Rwy	The principal wheel radii of curvature in the x and y- direction respectively.
Rrx & Rry	The principal wheel radii of curvature in the x and y- direction respectively
$\vec{R}_{pR}$	A vector defining the position of the wheel-rail contact point on the right rail
$\vec{R}_{pL}$	A vector defining the position of the wheel-rail contact point on the left rail
$\vec{R}_{rR}$	The global position vector defining the location of the origin of the local Car coordinate system.
T_{rR}	The transformation matrix
t_{rR}	The tangent unit vector.
ν	Poison's ratio

W_{pR}	*A vector defining the position of the wheel-rail contact point P on the right wheel.*
W_{pL}	*A vector defining the position of the wheel-rail contact point P on the left wheel.*
φ	*The angle between the principal planes is denoted.*
δ	*The elastic deformation (penetration depth) at the center of the contact patch*

1–INTRODUCTION

1.1. Background

Track geometry irregularity can be defined as the deviation of the constructed track geometry from the designed geometry and generally it will lead to passenger discomfort and wheel-rail contact stress problems.

The construction quality of a railway track covers a considerable impact on the serviceability of the whole railway project. Indeed it is difficult to have exactly the same designed geometries and constructed track geometries especially as long as labour based construction methodologies are being followed.

Therefore, in order to insure that the constructed railway network is safe and serviceable, including all the stipulated environmental, structural, operational, and economical standards have met by the constructed network, it is very important to give a considerable focus for the track irregularities and their effects on the serviceability and overall maintenance issues of the railway network.

1.2. Objective of the research

This research will focus on assessing the track geometry quality, track geometry deviations, and analyzing their effect on the wheel-rail contact relationship. The deviation of the actual constructed track from the designed geometry is known as track irregularity.

Specific objectives:

1. To detect the possible wheel rail contact point, involving mathematical analysis of rail surface and wheel thread geometry.

2. To analyze and point out the variation of the wheel-rail contact geometry, contact pressure and normal contact forces in the presence of the applied irregularities.

1.3 Methodology

1.3.1 General Approaches

In order to achieve the objectives of this thesis the following general methods will be employed:-

1. Developing the contact geometry relationship between the wheel and rail thereby calculating the possible coordinates for the wheel rail contact point.
2. After the contact geometry problem is solved, the calculated contact point will be applied to solve the elastic contact pressure problem based on Hertz theory for the one point contact problem.
3. Track system simulation, i.e. wheel and rail, using appropriate computer software will be conducted and then the possible track irregularities will be applied on the model. Finally, the results will be compared, i.e. contact point and contact forces, yielded from the above two stages.

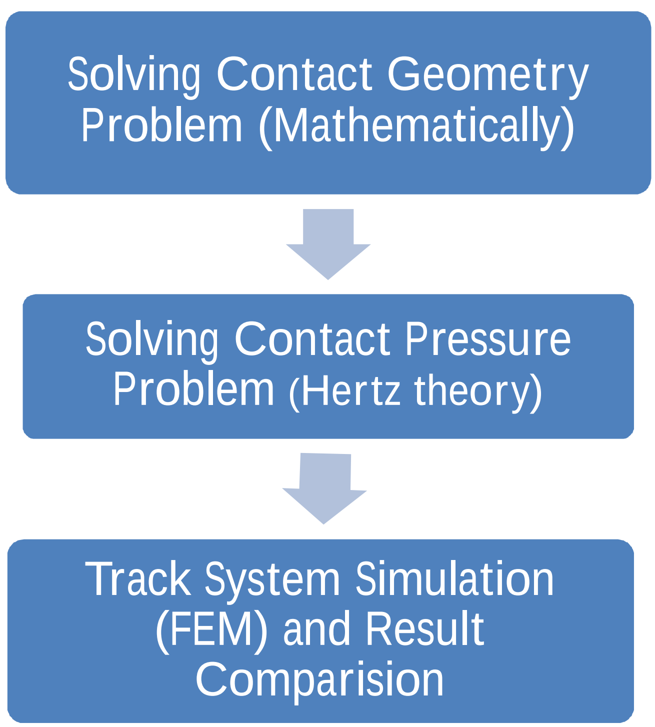

Figure 1.1- General methodology

1.3.2 Specific Approaches:-

1.3.2.1 Contact geometry determination:-

The detailed procedures of determining the contact geometry are as follows:-

Analysis of the rail surface geometries

Step 1: After determining the different coordinate systems, i.e. the global and the local coordinate system, the rail surface geometry will be analyzed.

Step 2: Drive an equation for the wheel rail contact point based on the predetermined coordinate systems.

Step 3: Define each components of the wheel rail contact point equation.

Step 4: Find the rail profile curve equation f(y) and its complete parametrized equation P(y).

Step 5: Find the tangent and normal unit vectors of the parameterized equation at the wheel rail contact point P.

Step 6: Finally write the wheel rail contact point equation in terms of a single variable y, i.e. lateral axis of the local coordinate system.

Step 7: Repeat the above six steps for the left rail.

Analysis of the wheel surface geometries

Step 1: The same procedure will be followed as in the rail surface geometry analysis.

Contact point determination

Step 1:- Equate the corresponding wheel and rail contact point equations, the results will be candidate coordinates of the wheel rail contact point P.

Step 2:- Screen out the candidates by setting boundary conditions based on the rail and wheel profile geometry using the assumption that there will only be a single wheel rail contact point P and. Generally, this may imply that the distance between the contact points on the wheel and on the rail is zero.

1.3.2.2 Normal contact force determination

In Hertz contact theory, due to the elastic deformation of the two profiled bodies, the common surface will attain an elliptic boundary [1]. Hertz contact theory is based on a number of assumptions; the two bodies in contact are regarded as half-spaces, where the contact area is small compared to the minimum dimensions of the bodies in contact. In addition, no plastic deformation in the contact patch is assumed, and the radii of curvature of wheel and rail profiles in the contact patch are assumed to be constant. It is clear that these are rough assumptions in cases of conformal contact and two-point contacts, which are common in turnout applications.

For example, for contacts near the gauge corner of the crossing rail, there is a significant variation of the wheel and rail profile curvatures within the contact patch and the dimensions of the contact patch may not be small compared to the radii of curvature of the contacting surfaces. In some cases, the half-space assumption is not valid when contact occurs close to the gauge corner. In this case, a non-elliptical contact area may govern.

According to Hertz theory, the normal pressure is distributed as an ellipsoid over the elliptic contact area with semi-axes a and b.

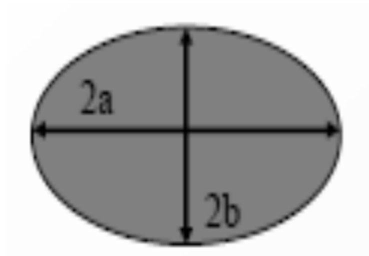

Figure1.2 Elliptic contact area

The ellipsoidal contact pressure distribution $P(x, y)$ is expressed by:-

$$P(x, y) = \frac{3F_n}{2\pi ab}\sqrt{1-\left(\frac{x}{a}\right)^2-\left(\frac{y}{b}\right)^2} \quad , \ldots \ldots \ldots \ldots \ldots \ldots \ldots \ldots \ldots \ldots (1.1)$$

Where:-

F_n= the normal contact force,

x and y = local coordinates with the origin at the center of the contact ellipse.

The x coordinate is bounded by the semi-axis a, $|x| \leq a$, and the y coordinate is bounded by the semi-axis b, $|y| \leq b$. according to the above equation the maximum pressure occurs at the center of the contact ellipse.

The semi-axes of the elliptic contact area are given by [2]:-

$$a = e\left[\frac{3\pi\, F_n(Kr+Kw)}{4\,(A+B)}\right]^{1/3} \quad \ldots\ldots\ldots\ldots\ldots\ldots\ldots\ldots(1.2)$$

$$b = n\left[\frac{3\pi\, F_n(Kr+Kw)}{4\,(A+B)}\right]^{1/3} \quad \ldots\ldots\ldots\ldots\ldots\ldots\ldots\ldots(1.3)$$

Where,

a = semi axis in the x direction.

b= semi axis in the y direction.

e & n = semi axis coefficients.

F_n = the normal contact force

According to the method in [2] A+B and B-A are parameters which defines the contact geometry. These parameters are dependent on the curvature of the two bodies in contact and on the angle between the principal axes and they are defined as follows:-

$$A+B=\frac{1}{2}\left(\frac{1}{Rrx}+\frac{1}{Rry}+\frac{1}{Rwx}+\frac{1}{Rwy}\right)\ldots\ldots\ldots\ldots\ldots\ldots\ldots \quad (1.4)$$

$$B-A=\frac{1}{2}\left[\left(\frac{1}{Rwx}-\frac{1}{Rwy}\right)^{2}+\left(\frac{1}{Rry}-\frac{1}{Rrx}\right)^{2}+ 2\left(\frac{1}{Rwx}-\frac{1}{Rwy}\right)\left(\frac{1}{Rrx}-\frac{1}{Rry}\right)\frac{cos2\varphi}{1}\right]^{1/2}\ldots\ldots\ldots\ldots \quad (1.5)$$

Where R_{WX} and R_{Wy} are the principal radii of curvature in the x- and y-directions of the wheel, and Rr_{X} and Rry are the principal radii of curvature in the x- and y-directions of the rail. The angle between the principal planes is denoted as φ.

2 - LITERATURE REVIEW

2.1 Track Geometry

2.1.1 Theoretical background

Track geometry is a general terminology used to describe the path and layout of the railway track by using different parameters [10]. Since the discussion is only about geometry, it is mandatory to form an appropriate coordinate system and the necessary sign conventions that will follow the pre-determined coordinate system. Accordingly, in order to describe the track system it will be appropriate to use a Cartesian coordinate system and the figure below will graphically describe the coordinate system.

Figure 2.1 Track's Global Coordinate System

For the sake of simplification, the origin of the coordinate system coincides with the center of the track. Therefore; the x-axis will be parallel to the ideal track centerline along the longitudinal direction of the track, with a positive direction in the direction of travel, the y-axis will be perpendicular to the track centerline and points to the left hand side of the transvers direction or in the lateral direction, and finally the z-axis points upward in the vertical direction or vertical axis.

2.1.2 Components of Railway Track Geometry

2.1.2.1 Track Gauge and Gauge widening

Track gauge is the distance between the inner sides of the two rails, measured 14mm below the rolling surface [11]. Across the globe there are three major types of track gauges. According to [11] they are defined as follows:-

Standard gauge = 1435mm:- Most lines have been laid at this gauge, found to optimize rolling stock dimensions. In standard gauge lines, the maximum permissible deviations from the 1435mm value range from the -3mm to +10mm.

Meter gauge = 1000mm:-Usually secondary lines are laid using meter gauge [11]. The meter gauges does not have high speed operation [12]. The maximum permissible deviation is -2mm to +3mm.

Broad gauge = 1524mm or 1672mm:-They have been constructed in order to differentiate them from the other types of gauge, mainly for political reasons, to prevent a rail vehicle which uses standard or meter gauge from passing into these networks.

Narrow gauge = 762mm [13] :- used for straight tracks including curves with radius up to 400m. The maximum permissible deviation is +3mm to -3mm.

In order to ease movement of vehicles and reduce wheel and rail wear, track gauge widening may be required in small radius curves [11]. Moreover, gauge widening application depends on the type of sleeper and track forms [12]. In addition, gauge widening should be avoided in turnouts [12].

2.1.2.2 Track Alignment

The track alignment has two components namely the horizontal alignment and vertical alignment. The projection of the track alignment on a horizontal plane is a horizontal alignment and the projection of the track alignment on a vertical plane is called vertical alignment.

The projection of a railway track centerline in a horizontal plane consists of three major components of tracks while traversing the railway line; tangents, Circular curves, and Transition curve.

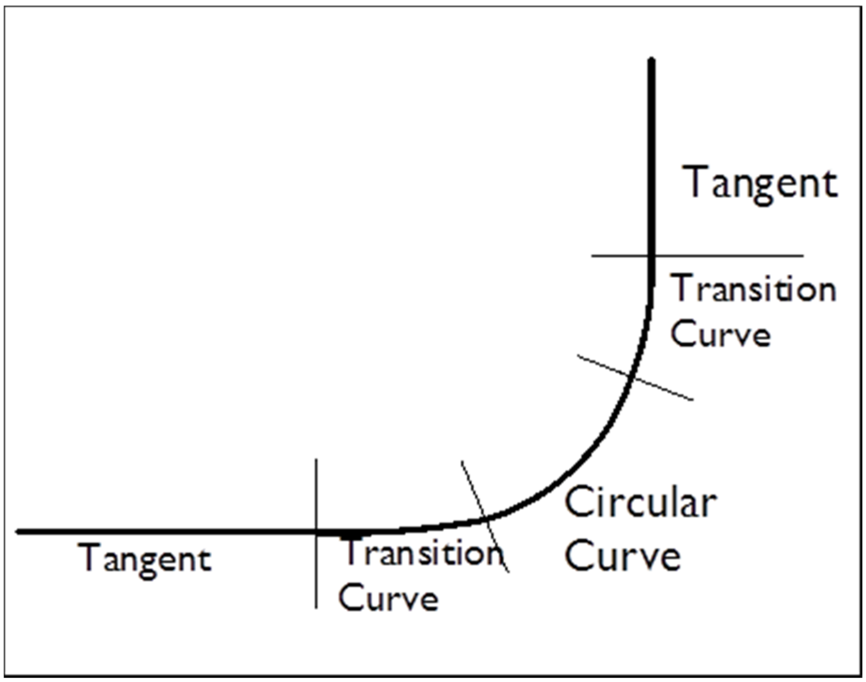

Figure 2.2 Components of horizontal alignment

As shown in Figure 2.2, tangent tracks are straight tracks and Circular curves are tracks with measurable curvature, or a fixed radius. The Transition curve is an easement curve, in which the change of radius is progressive throughout its length and is usually provided in a shape of a cubic parabola at each end of a circular curve to the section of the track that provides a smooth transition between tangents and curves, it does not have neither a fixed curvature nor curve radius.

A straight or a tangent track will have a zero horizontal curvature and will give us the shortest length between two points. According to [11] it is easy to install switches and crossings on the tangent track and since there is no quasi-static lateral acceleration, cant is not applied. Moreover, during designing the straight tracks there is no need to limit the maximum length rather due to various reasons it is important to set the minimum length.

A curved track is with a circular curve, i.e. constant curve radius R. If the train is running with a constant speed within a circular curve section then there will be a constant quasi-static lateral acceleration. Based on the speed of the line a minimum limitation is set for the radius of the curved tracks and also there is a minimum requirement for the track radius in platforms and turnouts. In addition the curve radius is indirectly proportional to the applied cant.

When the train is running in curved tracks with a constant radius R the following effects may be demonstrated [11]:-

- Possible passenger discomfort and noise,
- Possible displacement of wagon loads,
- Risk of vehicle overturning,
- Risk of derailment by wheel climbing or loosening of rail fastenings,
- High lateral forces on the track structure and substructure.

Transition curves can be used between straight tracks and curves and/or between two adjacent curves to allow gradual change in quasi-static lateral acceleration. It provides a gradual increase of curvature from zero at the tangent point to the specified radius and permits a gradual increase of cant, so that the full cant is attained simultaneously with the curvature of the circular arc. For the safety and comfort of the passengers it is preferred to use transition curves with a linear curvature changes.

As it is stated above a curved track will demonstrate certain kinds of phenomena that need to be mitigated. Therefore, raising the outer rail or superelevating the outer rail with a calculated amount, i.e. cant, will mitigate most of the above negative effects of applying a curved track.

The vertical alignment of a railway line consists of two components: constant gradient and vertical curves.

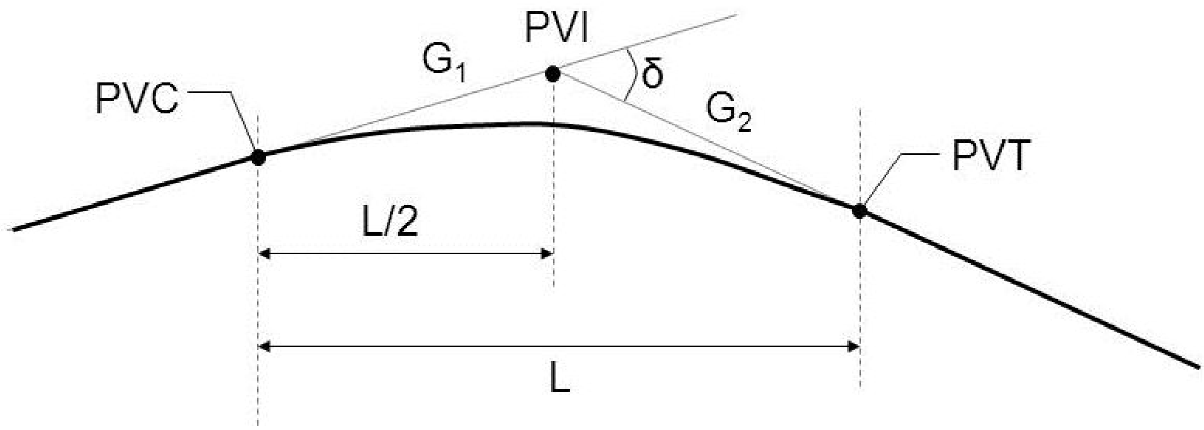

Figure 2.3 Vertical curve elements

The main purpose of providing gradient is to provide a uniform and comfortable rise or fall as far as possible. In addition, gradient is a departure from the horizontal level; a rising gradient is one when the track rises in the direction of movement, and a down or falling gradient is one when the track falls in the direction of movement [12].

The provided gradient may have a constant or non-constant rate. On the constant gradient there is no vertical curvature therefore there is no quasi-static vertical acceleration. Moreover, it is easy to install switches and crossing on the constant gradient section of the railway line [12]. The maximum gradient to be applied mainly depends on the characteristics and power of the rolling stock.

The purpose of applying a vertical curve on our railway designs is in order to maintain the wheel- rail contact, to ensure passenger comfort, and to guarantee good vision for communication purpose. A vertical curve provides a smooth transition between successive tangent gradients in the railway profile.

Within the vertical curved sections the gradient changes continuously as a function of the chainage. The length of vertical curve is associated with the rate of change of gradient, vertical acceleration, and the track speed. Moreover, the minimum vertical curve radius is associated with the track speed.

The most common type of vertical curve is the parabola, where the gradient changes linearly as a function of Chainage.

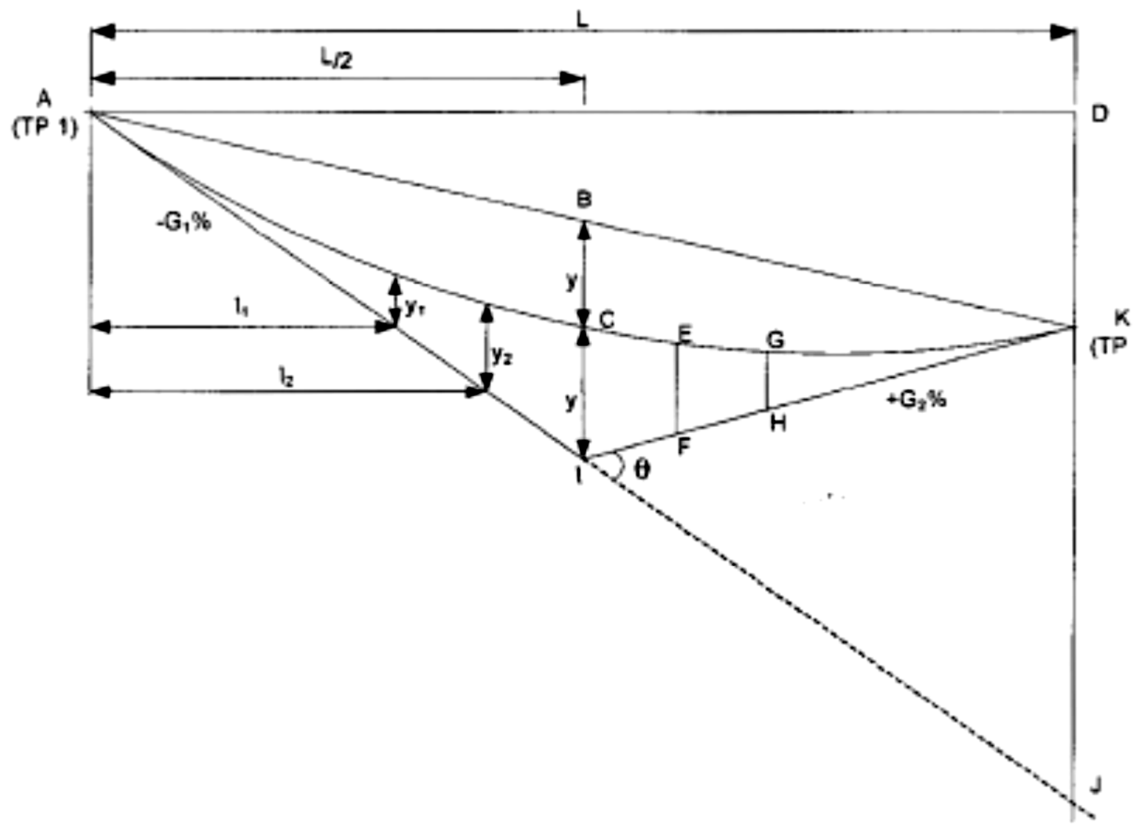

Figure 2.4 parabolic vertical curves

2.2 Track Irregularities

2.2.1 Introduction

Railway tracks are placed along a nominal centerline or path and this path is called ideal path of the track. Due to several reasons there will always be small deviations between geometric parameters of the constructed and designed ideal path. Accordingly, based on [11] track irregularity parameters are categorized into two; lateral and vertical parameters. The lateral parameters are described by track alignment and track gauge thereby represents the lateral deviations and the vertical parameters are described by profile and cross level thereby represents the vertical deviations.

2.2.2 Track Irregularity Parameters

2.2.2.1 Alignment Irregularity (Lateral)

The alignment irregularity is defined as the lateral deviation of the midpoint of the two rails from the nominal centerline of the track, shown in Figure 2.5. A positive deviation in the alignment denotes a lateral deviation of the track to the left, while a negative deviation in the alignment represents a lateral deviation of the track to the right. The left alignment and right alignment can be calculated as follows:-

$$\text{Left Alignment} = \frac{\text{Alignment} + \text{Gauge}}{2} \quad \text{(2.1)}$$

$$\text{Right Alignment} = \frac{\text{Alignment} - \text{Gauge}}{2} \quad \text{(2.2)}$$

$$\text{Alignment} = \frac{\text{Left Alignment} + \text{Right Alignment}}{2} \quad \text{(2.3)}$$

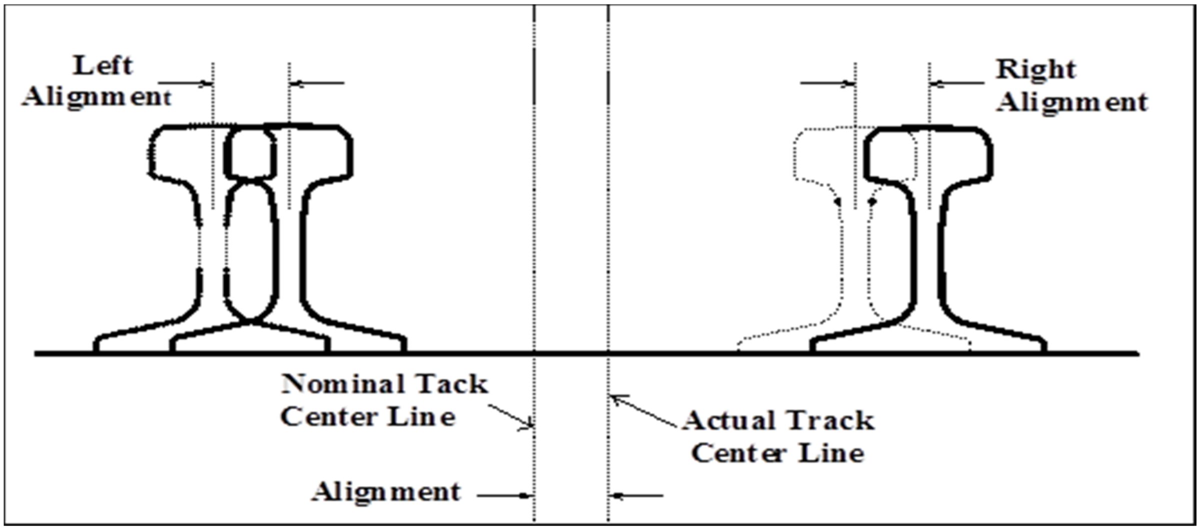

Figure 2.5 Track Alignment Deviations [10]

2.2.2.2 Gauge Irregularity (Lateral)

Gauge irregularity can be defined as the lateral deviation of the track from its nominal gauge, which is a standard gauge of width equal to 1435mm, as shown in Figure 2.6. It can be calculated as follows:-

Gauge = Actual gauge – Nominal Gauge………………. (2.4)

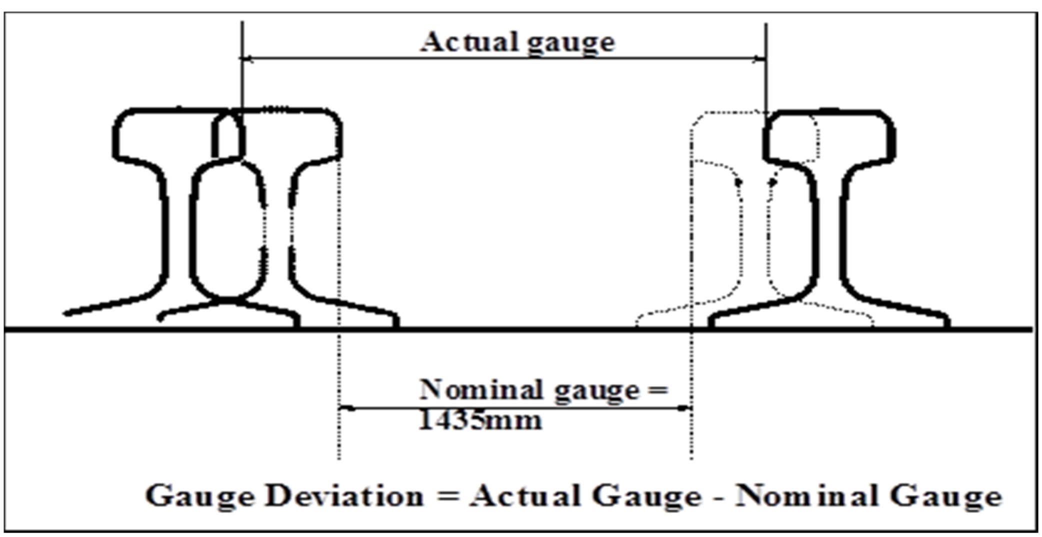

Figure 2.6 Track Gauge Deviations [10]

2.2.2.3 Cross Level (Vertical)

As illustrated in Figure 2.7 the cross level is the amount of vertical deviation between the left and right rail from their intended distance, the intended distance refers to the amount of cant used. For instance, if the cant is zero, then any difference between the elevations of the left and right rail is the cross level. If for instant the cant has a positive value, then the cross level is the deviation from this cant.

A positive cross level refers to the case when the left rail is above the right rail, and a negative cross level refers to an instance when the left rail is below the right rail. The cross level can be calculated using Equation (2.5).

Cross Level = Left Profile – Right Profile ------------- (2.5)

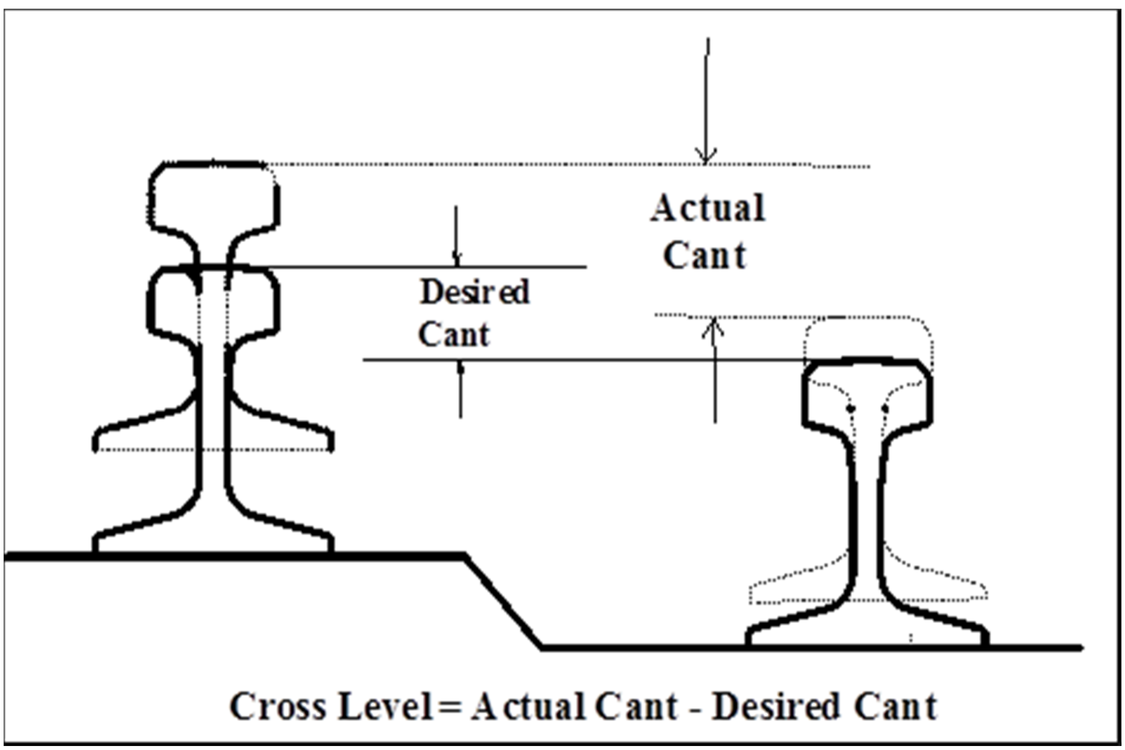

Figure 2.7 Track Cross Level Deviations [10]

2.2.2.4 Profile Irregularity (Vertical)

Profile irregularity is defined as the vertical deviation of the midpoint of the two rails from the track's nominal elevation, as shown in Figure 2.8.The left profile and right profile are the vertical deviations of each rail from its nominal path and can be calculated from the profile and cross level using equations 2.6 and 2.7.

$$\text{Left Profile} = \text{Profile} + \frac{\text{Cross Level}}{2} \quad \text{-----------------} \ (2.6)$$

$$\text{Right Profile} = \text{Profile} - \frac{\text{Cross Level}}{2} \quad \text{-----------------} \ (2.7)$$

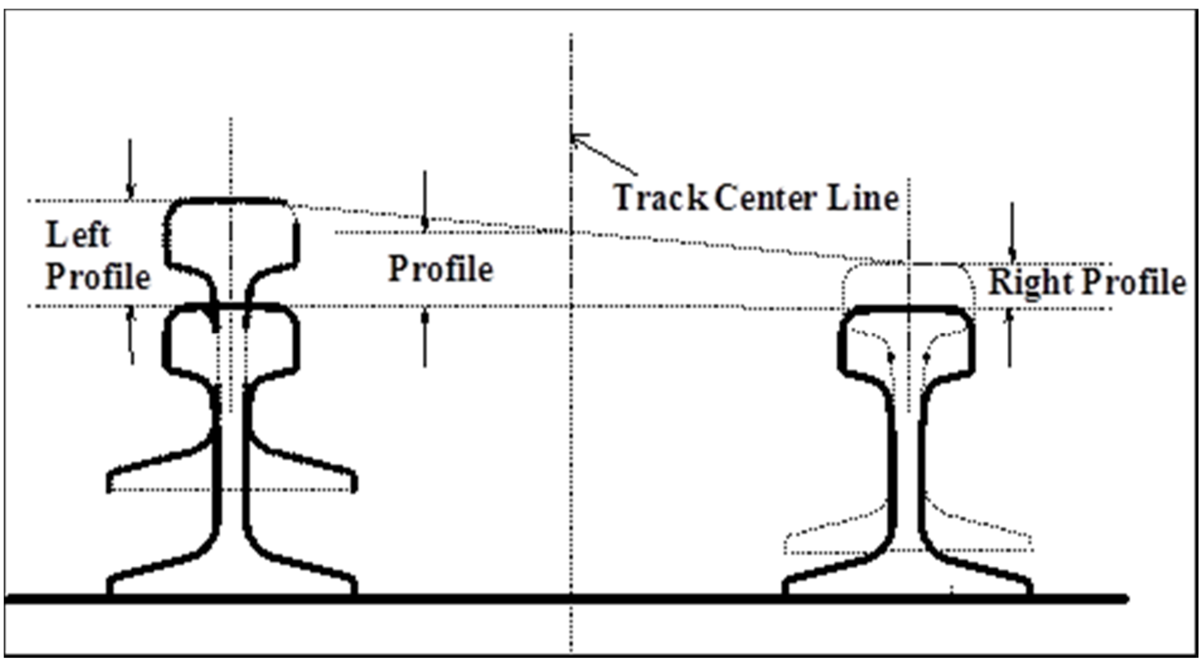

Figure 2.8 Track Profile Deviations [10]

2.3 International Standards

In this section track geometry parameters and qualities will be covered in accordance with standards, i.e. European norm (EN). In this paper track irregularities in the y- direction will be referred as lateral irregularities and irregularities in the z- direction will be referred as vertical irregularities.

2.3.1 Track Geometry Parameters (EN 13848 -1)

The European standard EN 13848-1 specifies the characteristics of the track geometry and defines different track geometry parameters. The different characteristics include track gauge, longitudinal level (vertical), cross level, alignment (lateral) and twist.

2.3.1.1 Track Gauge

According to [3] track gauge is defined as the smallest distance between lines perpendicular to track plane intersecting each railhead profile at point 14mm below the running surface. Nominal track gauges smaller than 1435 mm are called narrow gauges, and those wider than 1435mm are called broad gauges.

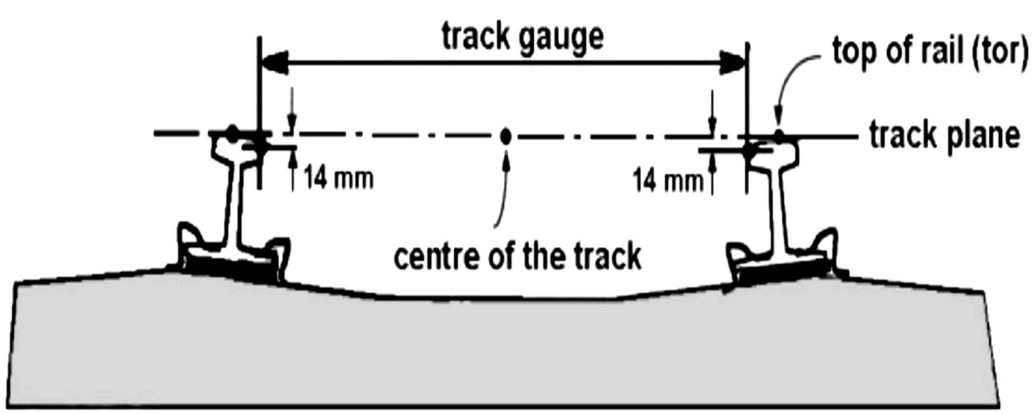

Figure 2.9 Track gauge

2.3.1.2 Longitudinal level (Vertical)

Standard longitudinal level is defined as a deviation of vertical elevation of top of rail, figure 2.9, and the value is expressed as a deviation from the mean vertical elevation [3]. This longitudinal level will cover the following wavelength ranges:

- Wavelength between 3-25 m, D1
- Wavelength between 25-70m, D2 and
- Wavelength between 70-150m, D3.

2.3.1.3 Cross Level (Cant)

Cross level is the measurement of the difference in elevation between the top surfaces of the two rails at any point of the railway track. The two points, each at the head of each rail, are measured at by the right angles to the reference rail.

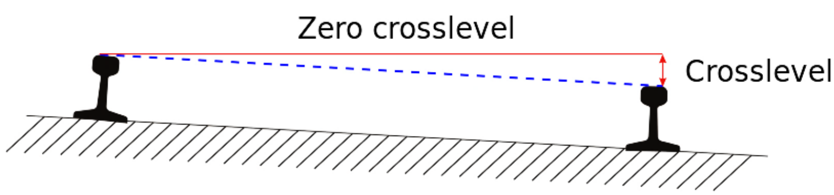

Figure 2.10 Cross level

It is said to be zero cross level when there is no difference in elevation of both rails. It is said to be reverse cross level when the outside rail of curved track has lower elevation than the inside rail.

Moreover, the speed limits are governed by the cross level of the track. In tangent track, it is desired to have zero cross level. However, the deviation from zero can take place. The cross level for curved track is called cant. Cant is applied in horizontal curve to decrease the lateral forces and make the curve more comfortable to pass through. This is achieved mainly because a larger part of the accelerations or forces are directed perpendicular to the track plane rather than parallel.

2.3.1.4 Alignment (Lateral)

Since track gauge is measured 14mm, i.e. Z_P, below the top fiber of the rail, and the lateral distance between the center line of the track and the point P is denoted as Y_p. Therefore, alignment irregularity is the deviation of the values between the actual measured Y_p and the designed value of Y_p.

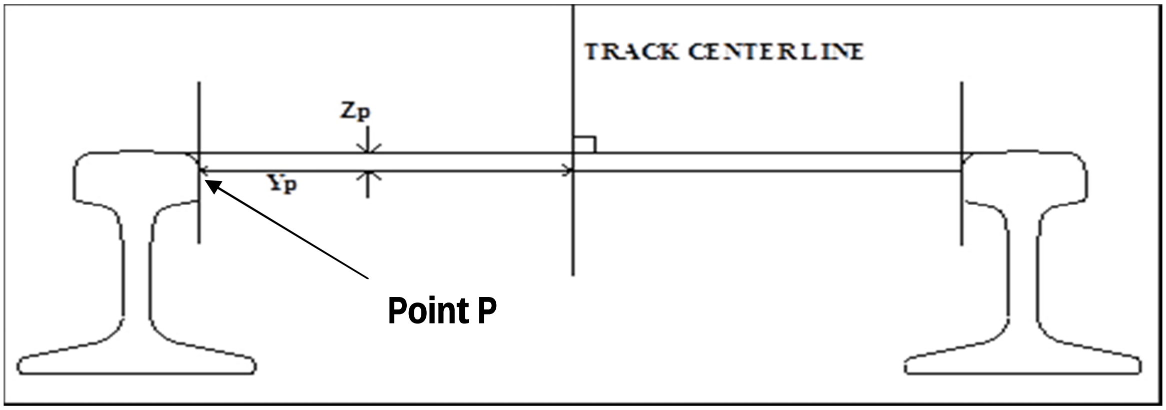

Figure 2.11 Lateral deviation

2.3.1.5 Twist

Twist is usually expressed as a gradient between two points of measurement which is taken at a defined distance apart. According to EN 13848-1 twist is the difference, algebraic, between two cross levels taken at the point of measurement.

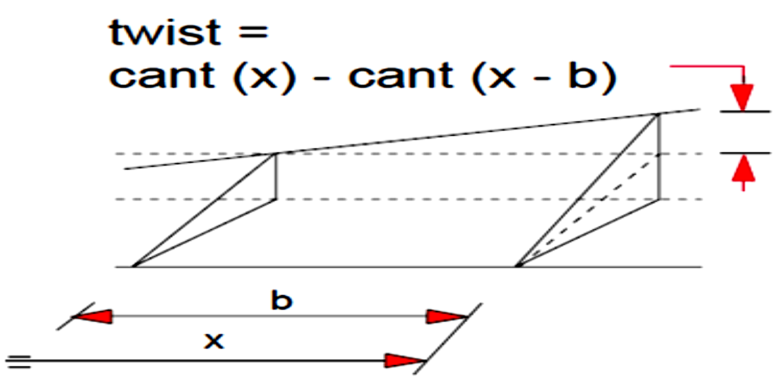

Figure 2.12 Twist

Twist can be expressed as a zero to peak or mean to peak value for isolated defects and it can be expressed in ‰ or mm/m.

2.3.2 Track geometry quality levels (EN 13848 -5)

EN 13848 -5 specifies the quality levels for the track geometry defined in 2.3.1. According to [4] there are three main quality levels which need to be considered:-

Immediate Action Limit (IAL): If a limit value is exceeded at this level, an action that corrects the error has to be done during the next scheduled maintenance [4].

Intervention Limit (IL): If a limit value is exceeded at this level, an action that corrects the error has to be done before the next inspection [4].

Alert Limit (AL): If a limit value is exceeded at this level, an action that lowers the risk of derailment has to be done immediately, i.e. maintenance, speed restrictions [4].

2.3.2.1Immediate action limits

This refers to the value which, if exceeded, requires taking measures to reduce the risk of derailment to an acceptable level. This can be done either by closing the line, reducing speed or by correction of track geometry. For the purpose of proper inspection and maintenance the standard clearly stipulates the limits for the track gauge, longitudinal level, cross level and alignment that will not need immediate remedial actions.

Track gauge

The values provided in the following tables apply to the nominal track gauge 1435mm, standard gauge.

Table 2.1 Track gauge –IAL- isolated Defects – Nominal track gauge to peak value [4]

Speed (in Km/h)	**Nominal track gauge to peak value (in mm) IAL**	
	Minimum	**Maximum**
V<= 80	-11	+35
80< V <= 120	-11	+35
120< V <= 160	-10	+35
160< V <= 230	-7	+28
230 < V <= 300	-5	+28

Longitudinal level

The values provided in the following tables apply to the nominal track gauge 1435mm, standard gauge.

Table 2.2 Longitudinal Level –IAL- isolated defects – mean to peak value [4]

Speed (in Km/h)	**Nominal track gauge to peak value (in mm) IAL**	
	Wavelength Range	
	D1	**D2**
V<= 80	28	N/A
80< V <= 120	26	N/A
120< V <= 160	23	N/A
160< V <= 230	20	33
230 < V <= 300	16	28

The mean, in the table above, is calculated over a length of at least twice the higher wavelength in the D1 or D2 range. In practice the mean will be close to zero and therefore zero to peak value may be used.

N.B:-For speeds less than or equal to 40 km/h, the limit can be relaxed to 31 mm.

Alignment and Cross level

This standard gives no IAL values for cross level because the risk associated with a cross level defect is tied to twist and cant deficiency. Cant deficiency limits depend on the track alignment design and construction rules, and the characteristics of the traffic, on each network. However, the standard gives IAL values for alignment.

Table 2.3 Alignment –IAL- isolated defects – mean to peak value [4]

Speed (in Km/h)	**Nominal track gauge to peak value (in mm) IAL**	
	Wavelength Range	
	D1	**D2**
V<= 80	22	N/A
80< V <= 120	17	N/A
120< V <= 160	14	N/A
160< V <= 230	12	324
230 < V <= 300	10	20

The mean, in the above table, is calculated over a length of at least twice the higher wavelength in the D1 or D2 range. In practice the mean will be close to zero and therefore zero to peak values may be used.

N.B:-**1.** For speeds less than or equal to 40 km/h, the limit can be relaxed to 31 mm.

2. Some types of track construction may have a greater risk of buckling when subject to high amplitude alignment defects; therefore a considerable attention needs to be given for the short wave defects with high amplitude.

2.3.2.2 Alert and Intervention limit

Unlike immediate action limits, which take into account the track-vehicle interaction, as well as the risk of unexpected events, the other quality levels are mainly linked with maintenance policy.

Therefore, track gauge, longitudinal level and alignment is discussed below with the help of tables taken from [4].

Track gauge

Table 2.4 Track gauge –AL & IL - isolated Defects – Nominal track gauge to peak value [4]

Speed (in Km/h)	Nominal track gauge to peak value (in mm) AL		Nominal track gauge to peak value (in mm) IL		Nominal track gauge to peak value (in mm) IAL (reminder)	
	Minimum	Maximum	Minimum	Maximum	Minimum	Maximum
V ≤ 80	-7	+25	-9	+30	-11	+35
80< V ≤ 120	-7	+25	-9	+30	-11	+25
120< V ≤160	-6	+25	-8	+30	-10	+35
160< V ≤ 230	-4	+20	-5	+23	-7	+28
230 < V ≤ 300	-3	+20	-4	+23	-5	+28

Longitudinal Level

Table 2.5 Longitudinal level –AL & IL - isolated Defects – Nominal track gauge to peak value [4]

Speed (in Km/h)	Nominal track gauge to peak value (in mm) AL		Nominal track gauge to peak value (in mm) IL		Nominal track gauge to peak value (in mm) IAL (reminder)	
	Wavelength range					
	D1	D2	D1	D2	D1	D2
V ≤ 80	12 to 18	N/A	17 to 21	N/A	28	N/A
80< V ≤ 120	10 to 16	N/A	13 to 19	N/A	26	N/A
120< V ≤160	8 to 15	N/A	10 to 17	N/A	23	N/A
160< V ≤ 230	7 to 12	14 to 20	9 to 14	18 to 23	20	33
230 < V ≤ 300	6 to 10	12 to 18	8 to 12	16 to 20	16	28

Table 2.6 Longitudinal level –AL – standard deviation [4]

Speed (in Km/h)	Standard Deviation (mm)
	Wavelength range –D1
V ≤ 80	2.3 to 3
80< V ≤ 120	1.8 to 2.7
120< V ≤160	1.4 to 2.4
160< V ≤ 230	1.2 to 1.9
230 < V ≤ 300	1 to 1.5

Alignment

Table 2.7 Alignment –AL & IL - isolated Defects – mean to peak value [4]

Speed (in Km/h)	Nominal track gauge to peak value (in mm) AL		Nominal track gauge to peak value (in mm) IL		Nominal track gauge to peak value (in mm) IAL (reminder)	
	Wavelength range					
	D1	D2	D1	D2	D1	D2
V ≤ 80	12 to 15	N/A	15 to 17	N/A	22	N/A
80< V ≤ 120	8 to 11	N/A	11 to 13	N/A	17	N/A
120< V ≤160	6 to 9	N/A	8 to 10	N/A	14	N/A
160< V ≤ 230	5 to 8	10 to 15	7 to 9	14 to 17	12	24
230 < V ≤ 300	4 to 7	8 to 13	6 to 8	12 to 14	10	20

Table 2.8 Alignment –AL – standard deviation [4]

Speed (in Km/h)	Standard Deviation (mm)
	Wavelength range –D1
V ≤ 80	2.3 to 3
80< V ≤ 120	1.8 to 2.7
120< V ≤160	1.4 to 2.4
160< V ≤ 230	1.2 to 1.9
230 < V ≤ 300	1 to 1.5

3 - ANALYSIS OF THE WHEEL AND RAIL SURFACE GEOMETRY

3.1 Rail Head Surface Geometry

Rails are steel girders placed end to end to provide a level and continuous surface for the movement of trains. The main purpose of using rail is to accommodate and distribute wheel loads that come from the train. Guiding the wheel in the lateral direction, providing a level and continuous surface for the movement of trains and distributing accelerating and breaking force by means of adhesion are other functions of rail.

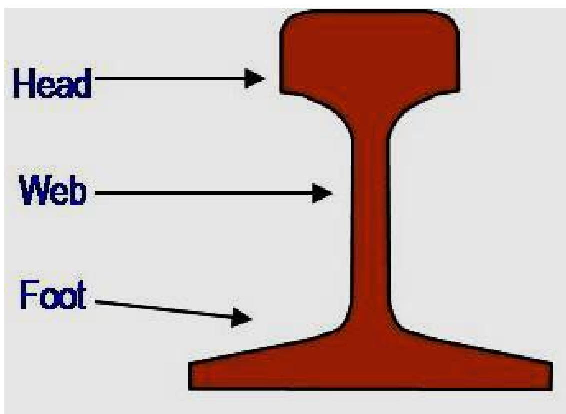

Figure 3.1 General (standard) rail Section

The rail is designated by its weight per unit length. The weight of the rail is expressed in metric units in kg per meter. The weight and section of the rail is governed by many factors, some of them are as follows; the gauge of the track, the maximum permissible speed of the train over the track, type and spacing of sleepers, and the heaviest moving load on the rail. Out of the above factors, the heaviest moving load is the most important factor.

In order to analyze the rail head geometry first different coordinate systems needs to be determined. Among the coordinate systems the first one is used to define the track system which is stated under section 2.1.1 figure 2.1 and the second one is a local profile coordinate system.

The global Cartesian coordinate system is composed of x, y and z axes in which the origin of the system coincides with the track centerline and accordingly the x-axis is parallel to the longitudinal track centerline and the y- axis is perpendicular to the track centerline which points transversally. And finally the z-axis points upward and also perpendicular to both the track centerline and transvers axis.

The local Cartesian coordinate system is used on both the left and the right rails defining the rail profile there by will help to identify the position and orientation of any cross section along the rail profile surface curve [5]. The origin of the local profile coordinate system lies on the rail head.

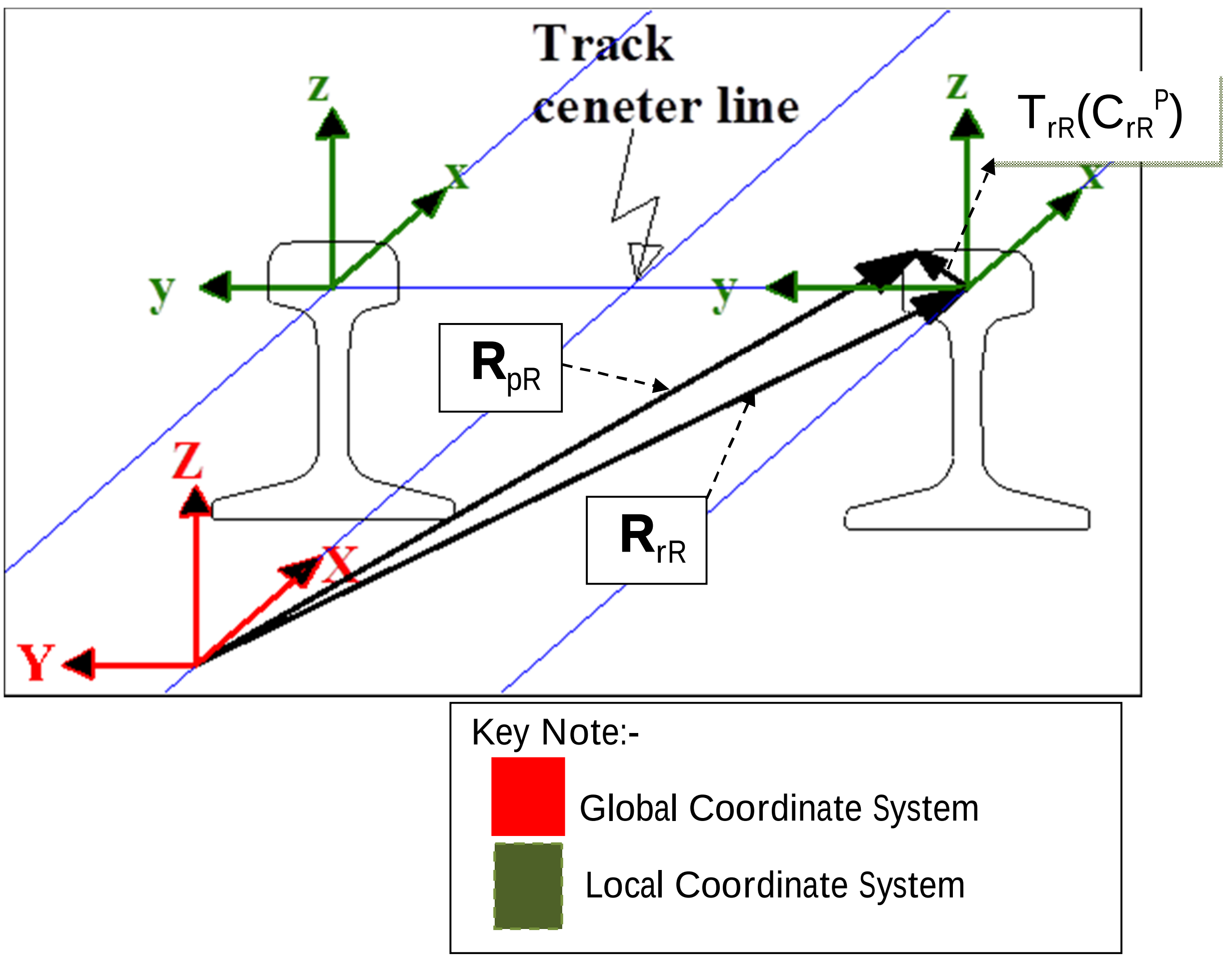

Figure 3.2 Global and Local Cartesian coordinate system [5]

According to [5] the profile coordinate system will define the arc length of the rail profile curve, C_r, and will give us the coordinate of the contact point as (x, y, z).

In order to account for the possible isolated track irregularities both the left and the right rails will be analyzed separately. Therefore, first the location of the wheel-rail contact point of the right rail will be derived.

$$\vec{R}_{pR} = \vec{R}_{rR} + T_{rR}(C_{rR}^{P}) \qquad (3.1)$$

Where:-

C_{rR}^{P} = local position vector defining the location of the contact point P with respect to the local coordinate system.

T_{rR} = the transformation matrix

$\vec{R}_{rR}$= the global position vector defining the location of the origin of the local coordinate system.

$\vec{R}_{pR}$= A vector defining the position of the wheel-rail contact point.

According to the pre-defined coordinate systems used to express the rail head surface geometry, the location of the origin of the local profile coordinate system is uniquely determined using the surface parameters and the contact point lies on the (y_{rR}, z_{rR}) plane. Consequently, in order to find the exact location of the wheel-rail contact point with respect to the global coordinate system, each components of equation 3.1 has to be explicitly defined.

Therefore, first it is necessary to define the global position vector, $\vec{R}_{rR}$, which will describe the local profile coordinate system's origin location. As it is stated earlier, for the purpose of this study the track gauge centerline coincides with the origin of the global Cartesian coordinate system. Subsequently, the x-components of the position vector $\vec{R}_{rR}$ will become zero and the y-coordinate will be the vertical distance across the rail cross section up to the origin of the local coordinate.

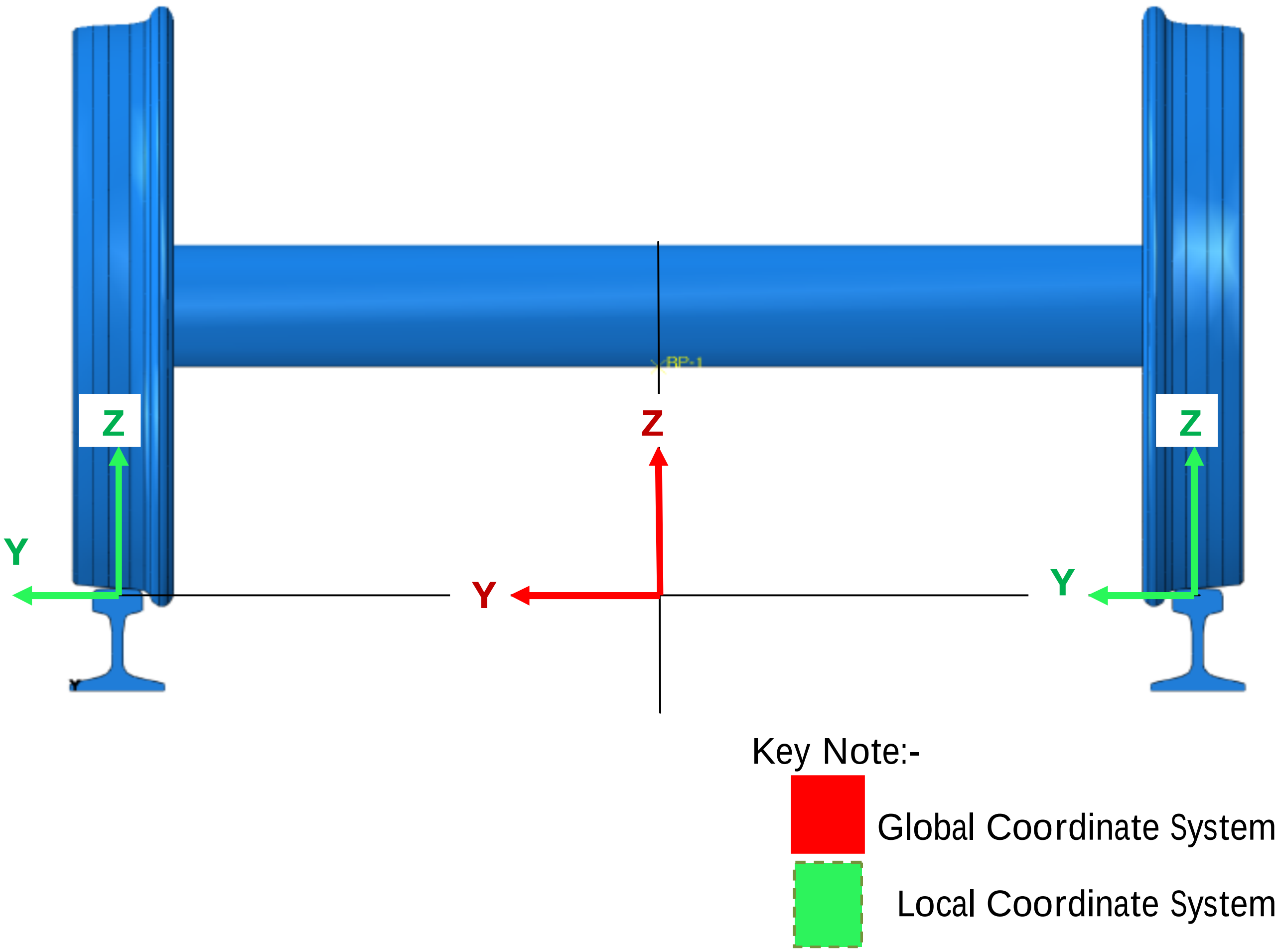

Figure 3.3 Simplified Coordinate systems

Hence:-

$$\vec{R}_{rR} = Xi + Yj + Zk$$

$$\vec{R}_{rR} = 0i + yj + 0k$$

$$\vec{R}_{rR} = -yj \text{-------------------------} \quad (3.2)$$

Second, the transformation matrix, T_{rR}, can be expressed using the tangential and the normal unit vectors, t_{rR} and n_{rR} respectively. These unit vectors define the moving reference frame associated with the right rail profile curve [5].

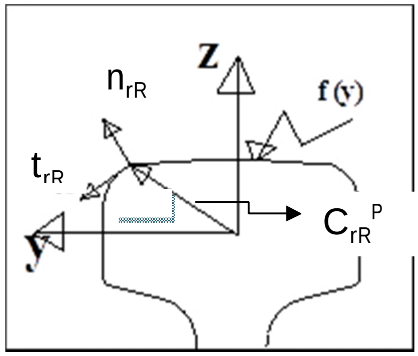

Figure 3.4 Components of the transformation matrix.

$T_{rR} = T_{rR}\ (C_{rR}^{p})$

$T_{rR} = [t_{rR}\ (C_{rR}^{p})\ n_{rR}\ (C_{rR}^{p})]$ ----------------- (3.3)

Since C_{rR}^{P} is a local position vector defining the location of the contact point P with respect to the local coordinate system and also P lies only on the y- z plane, therefore C_{rR}^{P} can be written as :-

$C_{rR}^{P} = \{ 0, y_{rR}, z_{rR}\}^{T}$, and $Z_{rR}= f(y_{rR})$;

$$C_{rR}^{P} = \begin{vmatrix} 0 \\ y_{rR} \\ f(y_{rR}) \end{vmatrix} \text{ ---------------------------- } (3.4)$$

Before proceeding to the next step, i.e. computing the tangential and normal components of the transformation matrix, it is mandatory to parametrized the rail profile curve equation, f(y), and the parametrized equation will be denoted by P(y).

For the purpose of this thesis rail with 50 kg/m will be used for a geometric analysis. Therefore, the national standard of the people's republic of china [6] specifies the selected sections geometry as follows:-

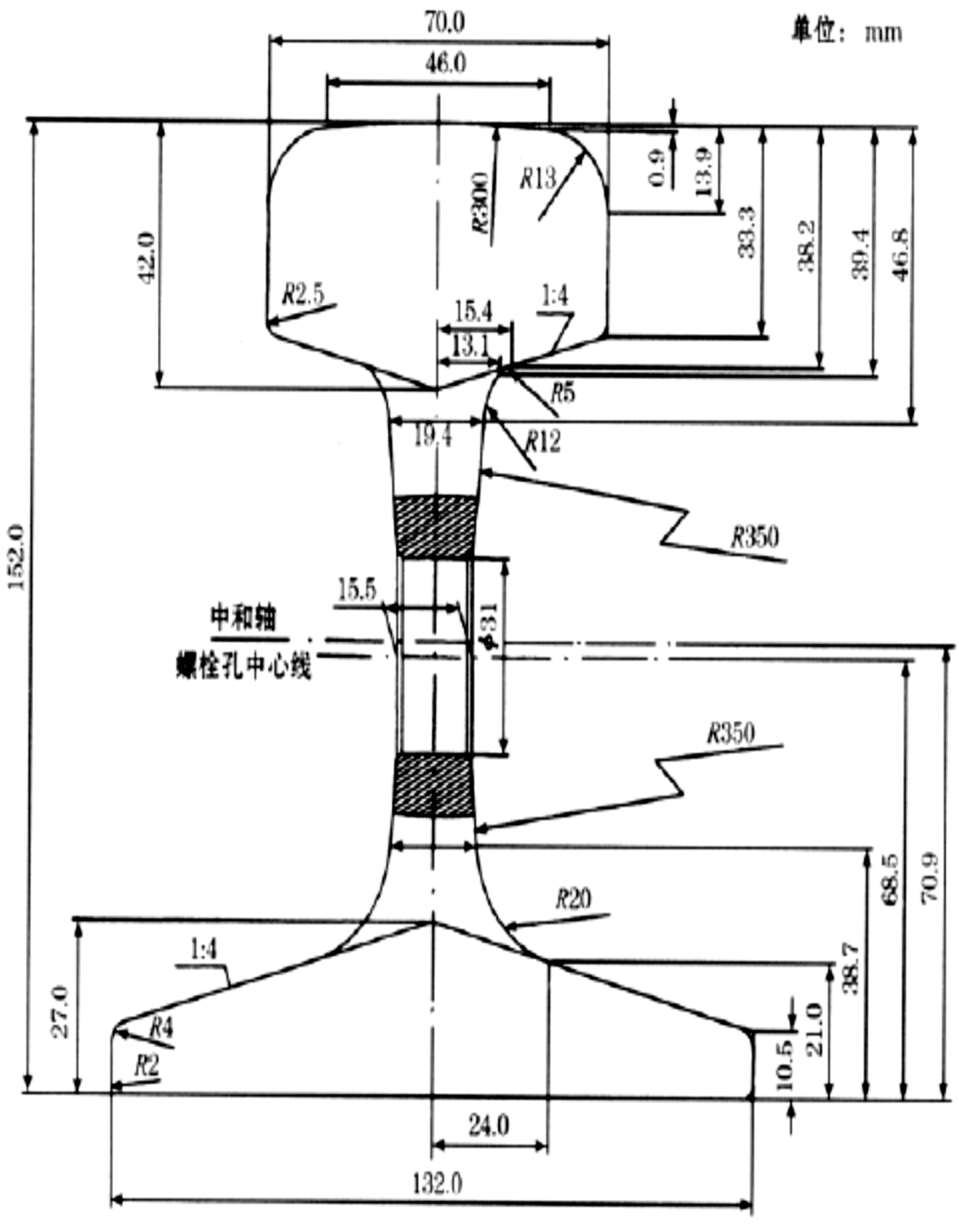

Figure 3.5 Rail profile for 50kg/m. Adapted from [6].

Moreover, the rail head is divided into three different contact regions as shown in the figure 3.7 below.

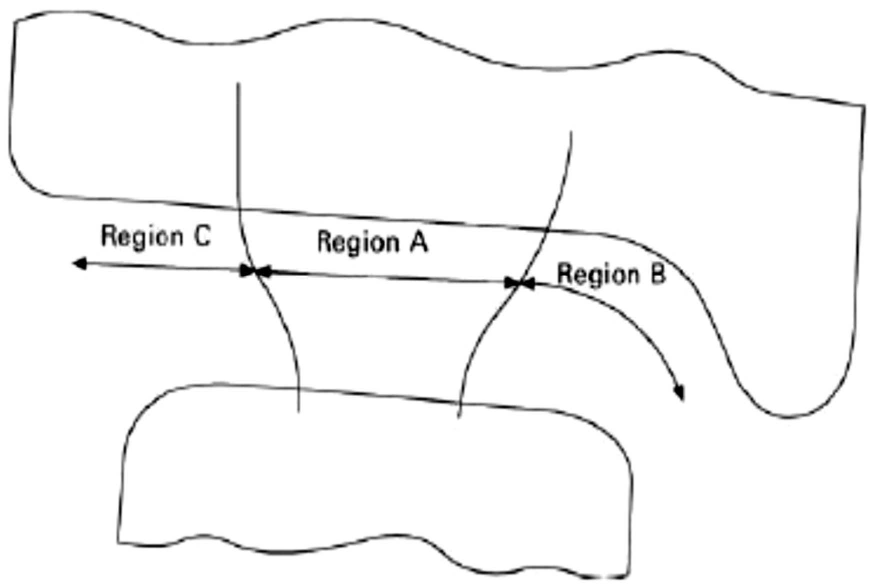

Figure 3.6 wheel-rail contact zones. Adapted from [12].

Region A is called wheel tread-rail head contact. It is the most common contact region and has a lower contact stress. Region B is called wheel flange – rail gauge corner. It has a much smaller contact area and more severe, i.e. higher contact stresses and wears rates. Region C is called wheel and rail field sides contact. It is a least likely contact region, higher contact stress and it shows undesirable wear which will lead to incorrect steering of wheelset.

Based on the information provided in the above paragraph for this thesis the wheel – rail contact problems will be computed by assuming that the contact region will be within Region A. Therefore, according to the Chinese standard, figure 3.5, the geometry of region A is specified as a circle with radius of 300mm and the center of the circle is situated 300mm below the top rail head surface.

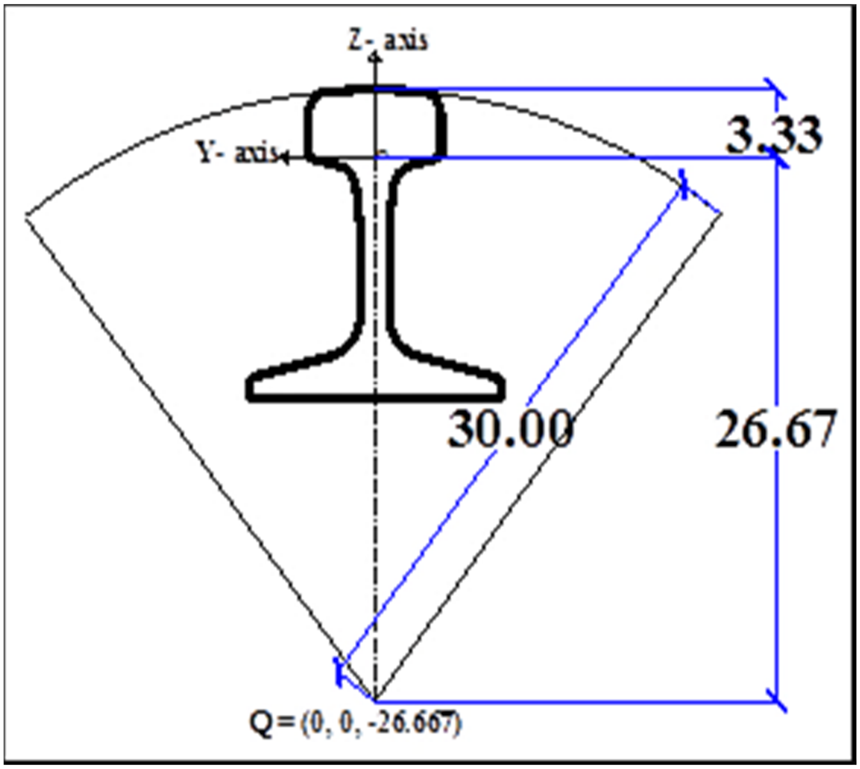

Figure 3.7 Rail profile Equation development

From figure 3.7 the coordinate for the center of the circle Q is (0, 0, -26.67), Since the circle is on the y-z plane it is enough to use the values of y and z coordinate of the center of the circle, i.e. (0, -26.67), subsequently the equation of the circle will become :-

$$Y^2 + (z + 26.67)^2 = 30^2 \text{------------------------------------} (3.5)$$

Since our aim is to find the tangent and normal unit vectors for the rail profile curve at the contact point P, parametrization of the profile curve stated on equation 3.5 will be commenced as follows:-

$$P = \{y, z\} \text{--} (3.6)$$

The coordinates y and z in the above equation are not arbitrary rather they are related through equation 3.5. This means that one can freely assign a value to only one of the coordinates, i.e. y, and then the value for the other coordinate, i.e. z, will be determined from the equation of the circle provided in equation 3.5.

Choosing y as the parameter for the curve, z can be written as:-

$$z = \pm\sqrt{30^2 - y^2} \text{ - } 26.67 \text{ ------------------------------- } (3.7)$$

Finally, the complete parametrization of the rail profile curve, f(y), becomes:-

$$P(y) = (y,\ \pm\sqrt{30^2 - y^2} \text{ - } 26.67) \text{ ----------------------- } (3.8)$$

OR

$$P_1(y) = yj + \sqrt{30^2 - y^2} \text{ - } 26.67k \text{ -------------------- } (3.9)$$

$$P_2(y) = yj - \sqrt{30^2 - y^2} \text{ - } 26.67k \text{ -------------------- } (3.10)$$

Where, the positive square root, equation 3.9, describes those points on the curve that lies above the y-axis and the negative square root describes the points lie below the y-axis. Therefore, since the rail head curve is above the y-axis, equation 3.9 will become the valid parametrized equation for the rail head curve within region A of the contact area.

Equation 3.9 represents the rail head profile curve, the smooth curve within the contact region A, by P(y). Then the unit tangent vector **t(y)** for the same curve is defined as:-

$$t(y) = \frac{\mathbf{P'(y)}}{//\mathbf{P'(y)}//}\ \mathbf{,}\ P'(y) \neq 0 \text{-------------------- } (3.11)$$

Where:

t(y) = is the unit tangent vector for the parametrized rail head curve.
P'(y) = the first derivatives of the parametrized equation.
//P'(y)// = the magnitude of the P'(y) vector.

$$P'(y) = j- \frac{y}{\sqrt{30^2-y^2}}k \text{ -- (3.12)}$$

$$//P'(y)// = \sqrt{1 + (\frac{y^2}{30^2- y^2})}$$

$$//P'(y)// =\frac{30}{\sqrt{30^2-y^2}} \text{ -- (3.13)}$$

Therefore, the unit tangent vector becomes:-

$$\mathbf{t(y) = 0}\ \boldsymbol{i} + \frac{\sqrt{\mathbf{30^2- y^2}}}{\mathbf{30}}\ \mathbf{j} + \frac{\boldsymbol{y}}{\mathbf{30}}\mathbf{k} \text{ ---------------------------- (3.14)}$$

For the parametrized curve P(y) the principal unit normal vector n(y) is defined as:-

$$n(y)= \frac{\mathbf{t\prime(y)}}{//\mathbf{t\prime(y)}//}\ \mathbf{,}\ t'(y) \neq 0 \text{ -----------------------(3.15)}$$

Where:

n(y) = is the unit normal vector for the parametrized rail head curve.
t'(y) = the first derivatives of the unit tangent vector.
//t'(y)// = the magnitude of the t'(y) vector.

$$t'(y) =\frac{1}{30}\left(- \frac{y}{\sqrt{30^2-y^2}}j + k\right) \text{ -------------------------------------- (3.16)}$$

$$//t'(y)// = \frac{1}{30}\left(\sqrt{\left(\frac{y^2}{30^2- y^2}\right) + 1}\right) \text{ -------------------------------- (3.17)}$$

$$//t'(y)// = \frac{1}{\sqrt{30^2 - y^2}} \quad \text{---} \ (3.18)$$

Therefore, the unit tangent vector becomes:-

$$\mathbf{n(y)} = 0i - \frac{y}{30}\mathbf{j} + \frac{\sqrt{30^2 - y^2}}{30}\mathbf{k} \text{-----------------------------} \quad (3.19)$$

- t_{rR} (C_{rR}) = (ti tj tk) (0 y f(y))

$$t_{rR}(C_{rR}) = \begin{vmatrix} ti\,(0) & ti\,y & ti\,f(y) \\ tj\,(0) & tj\,y & tj\,f(y) \\ tk\,(0) & tk\,y & tk\,f(y) \end{vmatrix}$$

$$t_{rR}(C_{rR}) = \begin{vmatrix} 0 & ti\,y & ti\,f(y) \\ 0 & tj\,y & tj\,f(y) \\ 0 & tk\,y & tk\,f(y) \end{vmatrix} \text{-----------} \ (3.20)$$

- n_{rR} (C_{rR}) = (ni nj nk) (0 y f(y)), and following the same procedure as for the tangent :-

$$n_{rR}(C_{rR}) = \begin{vmatrix} 0 & ni\,y & ni\,f(y) \\ 0 & nj\,y & nj\,f(y) \\ 0 & nk\,y & nk\,f(y) \end{vmatrix} \text{-------------} \ (3.21)$$

Where :-

t_{rR} = tangent unit vector for the profile function f(y) at the wheel rail contact point P.

n_{rR}= normal unit vector for the profile function f(y) at the wheel rail contact point P.

The transformation matrix becomes:-

$$T_{rR}(C_{rR})= \begin{vmatrix} 0 & ti\ y & ti\ f(y) \\ 0 & tj\ y & tj\ f(y) \\ 0 & tk\ y & tk\ f(y) \end{vmatrix} \begin{vmatrix} 0 & ni\ y & ni\ f(y) \\ 0 & nj\ y & nj\ f(y) \\ 0 & nk\ y & nk\ f(y) \end{vmatrix}$$

$$T_{rR}(C_{rR})= \begin{vmatrix} 0 & ti\ y^2(ni+nj+nk) & ti\ f(y)^2(ni+nj+nk) \\ 0 & tjy^2(ni+nj+nk) & tj\ f(y)^2(ni+nj+nk) \\ 0 & tky^2(ni+nj+nk) & tk\ f(y)^2(ni+nj+nk) \end{vmatrix} \text{ --------- (3.22)}$$

Finally, at this stage, components of equation 3.1can be fully written, i.e. the equation for the contact point P,

From equation 3.1:-

$$R_{pR}=R_{rR}+ T_{rR}(C_{rR}{}^{P})$$

From equation 3.2:-

$$R_{rR} =-yj$$

From equation 3.22:-

$$T_{rR}(C_{rR}{}^{P})= \begin{vmatrix} 0 & ti\ y^2(ni+nj+nk) & ti\ f(y)^2(ni+nj+nk) \\ 0 & tjy^2(ni+nj+nk) & tj\ f(y)^2(ni+nj+nk) \\ 0 & tky^2(ni+nj+nk) & tk\ f(y)^2(ni+nj+nk) \end{vmatrix}$$

From Equation 3.14

$$t(y) = 0i +\frac{\sqrt{30^2- y^2}}{30}\,j + \frac{y}{30}k$$

From equation 3.19:-

$$n(y) = 0i- \frac{y}{30}\,j + \frac{\sqrt{30^2- y^2}}{30}k$$

From equation 3.7:-

$$f(y) = \sqrt{30^2 - y^2} - 26.67$$

Therefore by letting m = $\sqrt{30^2 - y^2}$, and u = $\frac{y}{30}$ equation 3.22 can be simplify as follows:-

$$T_{rR}(C_{rR}^{P}) = \begin{vmatrix} 0 & ti\, y^2(ni+nj+nk) & ti\, f(y)^2(ni+nj+nk) \\ 0 & tjy^2(ni+nj+nk) & tj\, f(y)^2(ni+nj+nk) \\ 0 & tky^2(ni+nj+nk) & tk\, f(y)^2(ni+nj+nk) \end{vmatrix}$$

$$T_{rR}\,(C_{rR}^{P}) = \begin{vmatrix} 0 & (0)(y^2)(0 - u + \frac{m}{30}) & (0)(m-26.67)^2\,(0 - u + \frac{m}{30}) \\ 0 & (\frac{m}{30})(y^2)(0 - u + \frac{m}{30}) & (\frac{m}{300})(m-26.67)^2(0 - u + \frac{m}{30}) \\ 0 & (u)(y^2)(0 - u + \frac{m}{30}) & (u)(m-26.67)^2(0 - u + \frac{m}{30}) \end{vmatrix} \text{-------- (3.23)}$$

Therefore the final equation for the ***right rail*** become:-

$$\mathbf{R_{pR} = -yj +} \begin{vmatrix} \mathbf{0} & \mathbf{0} & \mathbf{0} \\ \mathbf{0} & \mathbf{(\frac{m}{30})(y^2)(-u+\frac{m}{30})} & \mathbf{(\frac{m}{30})(m-26.67)^2(-u+\frac{m}{30})} \\ \mathbf{0} & \mathbf{(u)(y^2)(-u+\frac{m}{30})} & \mathbf{(u)(m-26.67)^2(-u+\frac{m}{30})} \end{vmatrix} \text{--- (3.24)}$$

And for the ***left rail*** the above equation will become:-

$$\mathbf{R_{pL} = yj +} \begin{vmatrix} \mathbf{0} & \mathbf{0} & \mathbf{0} \\ \mathbf{0} & \mathbf{(\frac{m}{30})(y^2)(-u+\frac{m}{30})} & \mathbf{(\frac{m}{30})(m-26.67)^2(-u+\frac{m}{30})} \\ \mathbf{0} & \mathbf{(u)(y^2)(-u+\frac{m}{30})} & \mathbf{(u)(m-26.67)^2(-u+\frac{m}{30})} \end{vmatrix} \text{------ (3.25)}$$

3.2 Wheel Surface Geometry

For analyzing the wheel surface geometry the same approach will be followed as for the rail surface geometry analysis. Therefore, first an equation for the wheel-rail contact point, P, of the right wheel will be derived.

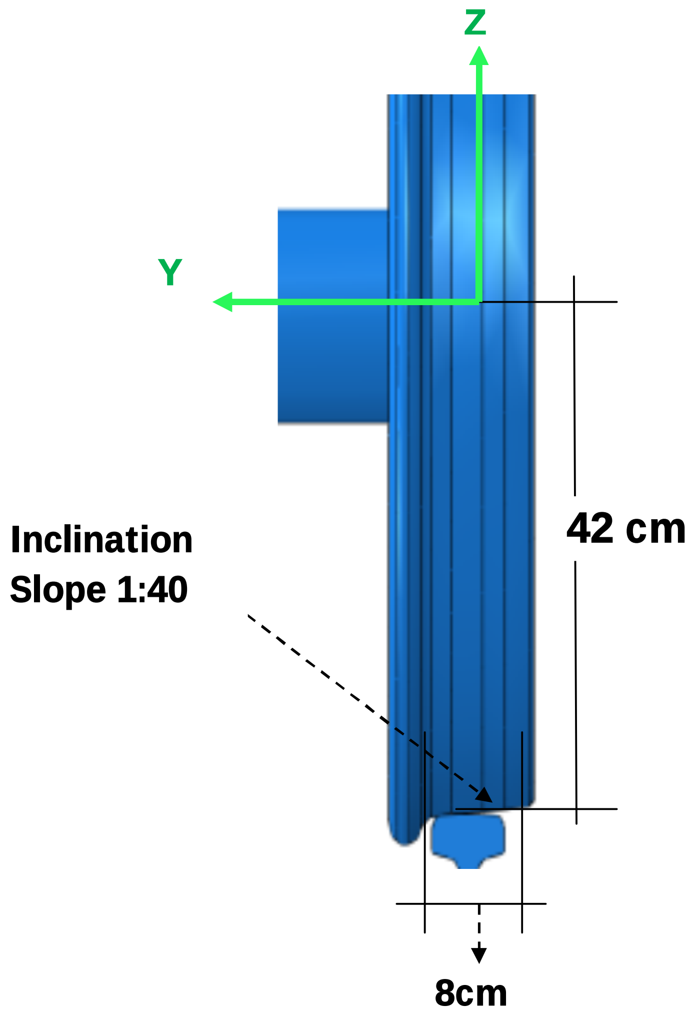

Figure 3.8 wheel geometry

As in the case for section 3.1both the left and the right wheels will be analyzed separately. An equation for the location of the wheel-rail contact point, P_w, of the right wheel can be written as follows:-

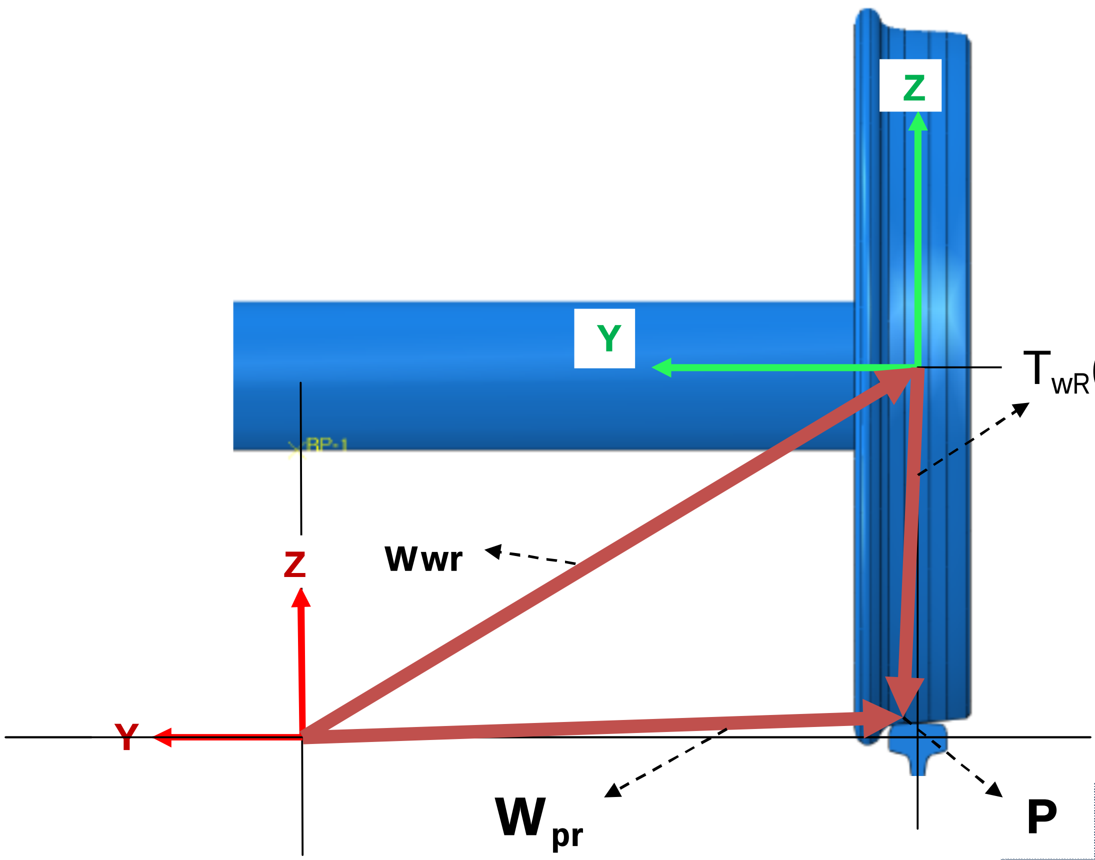

Figure 3.9 wheel surface parametrization

$$\vec{W}_{pR}=\vec{W}_{wR}+T_{wR}(C_{wR}{}^{P}) \text{ ------------------------------------ } (3.26)$$

Where:-

$C_{wR}{}^{P}$ = local position vector defining the location of the contact point P with respect to the local coordinate system.

T_{wR} = the transformation matrix

$\vec{W}_{wR}$= the global position vector defining the location of the origin of the local profile coordinate system.

$\vec{W}_{pR}$= A vector defining the position of the wheel-rail contact point.

The global position vector defining the location of the origin of the local profile coordinate system, $\vec{W}_{wR}$,:-

$$\vec{W}_{wR}= Xi + Yj + Zk$$

$$W_{wR} = 0i - yj + zk$$

$$\vec{W}_{wR} = 0i - yj + \mathbf{z}k \text{ ------------------------- } (3.27)$$

Second, the transformation matrix T_{rR} can be expressed using the tangential and the normal unit vectors, t_{wR}, and n_{wR} respectively.

$$T_{wR} = T_{wR}\,(C_{wR}^{p})$$
$$T_{wR} = [t_{wR}(C_{wR}^{p})\ n_{wR}\,(C_{wR}^{p})\ ] \text{ ---------------- } (3.28)$$

$C_{wR}^{P} = \{\,0,\, y_{wR},\, z_{wR}\}^{T}$, and $Z_{wR} = f(y_{wR})$;

$$C_{wR}^{P} = \begin{vmatrix} 0 \\ y_{wR} \\ f(y_{wR}) \end{vmatrix} \text{ --------------------------- } (3.29)$$

Since the wheel rail contact point lies at the thread of the wheel surface, the geometry of the wheel thread will only be considered.

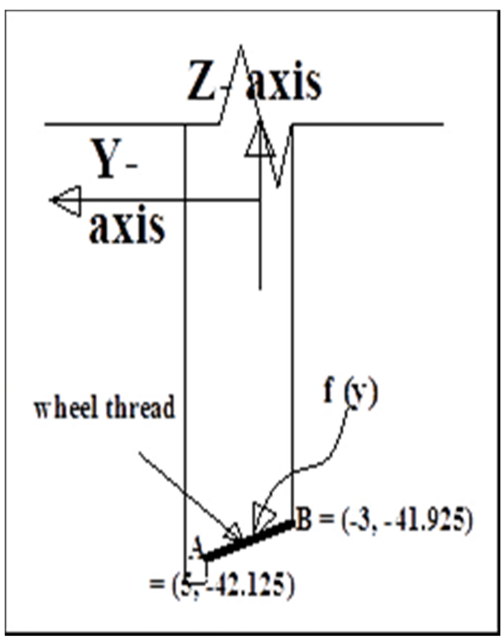

Figure 3.10 wheel thread section.

In order to compute the tangential and normal components of the transformation matrix the wheel thread function f(y) and its parametrized equation P(y) has to be determined first.

Since the wheel thread is an inclined straight line, in order to find its equation, f(y), two coordinate points that needs to be on the thread, will be used, i.e. point A and point B of figure 3.11.The two coordinate points on the wheel thread line will be measured from the local wheel coordinate system, i.e. A= (0, 5, -42.125) and B= (0, -3, -41.925), therefore the equation f(y) becomes:-

f(y) = - 0.025 y – 42 ------------------------------------- (3.30)

Then the complete parametric equation will be:-

P(y) = yj – (0.025 y +42)k ------------------------------ (3.31)

Then the unit tangent vector **t(y)** is defined as:-

$$t(y) = \frac{\mathbf{P'(y)}}{//\mathbf{P'(y)}//}, \; P'(y) \neq 0 \text{ --------------------- } (3.32)$$

Where:

t(y) = is the unit tangent vector for the parametrized wheel thread.
P'(y) = the first derivatives of the parametrized equation.
//P'(y)// = the magnitude of the P'(y) vector.

P'(y) = j –(0.025) k -- (3.33)

//P'(y)// = 1.00 -- (3.34)

Therefore, the unit tangent vector becomes:-

t(y) = 0i + j - 0.025k----------------------------- (3.35)

Hence, the unit normal vector becomes:-

$$\mathbf{n(y) = 0i - 0.025\,j - k} \text{-----------------------------} \qquad (3.36)$$

- $t_{wR}\,(C_{wR}) = (ti\ \ tj\ \ tk)\,(0\ \ y\ \ f(y))$

$$t_{wR}\,(C_{wR}) = \begin{vmatrix} 0\,(0) & 0\,y & 0\,f(y) \\ tj\,(0) & tj\,y & tj\,f(y) \\ tk\,(0) & tk\,y & tk\,f(y) \end{vmatrix}$$

$$t_{wR}\,(C_{wR}) = \begin{vmatrix} 0 & 0 & 0 \\ 0 & tj\,y & tj\,f(y) \\ 0 & tk\,y & tk\,f(y) \end{vmatrix} \text{-----------} \ (3.37)$$

- $n_{wR}\,(C_{wR}) = (ni\ \ nj\ \ nk)\,(0\ \ y\ \ f(y))$, and following the same procedure as for the tangent :-

$$n_{wR}(C_{wR}) = \begin{vmatrix} 0 & 0 & 0 \\ 0 & nj\,y & nj\,f(y) \\ 0 & nk\,y & nk\,f(y) \end{vmatrix} \text{-------------} \ (3.38)$$

Where:-

t_{wR} = tangent unit vector for the profile function f(y) at the wheel rail contact point P_w.

n_{wR}= normal unit vector for the profile function f(y) at the wheel rail contact point P_w.

The transformation matrix becomes:-

$$T_{wR}(C_{wR}) = \begin{vmatrix} 0 & 0 & 0 \\ 0 & tj\,y & tj\,f(y) \\ 0 & tk\,y & tk\,f(y) \end{vmatrix} \begin{vmatrix} 0 & 0 & 0 \\ 0 & nj\,y & nj\,f(y) \\ 0 & nk\,y & nk\,f(y) \end{vmatrix}$$

$$T_{wR}(C_{wR}) = \begin{vmatrix} 0 & 0 & 0 \\ 0 & tjy^2(ni+nj+nk) & tj\, f(y)^2(ni+nj+nk) \\ 0 & tky^2(ni+nj+nk) & tk\, f(y)^2(ni+nj+nk) \end{vmatrix} \text{---------} \quad (3.39)$$

Finally, at this stage, components of equation 3.1 can be fully written, i.e. the equation for the contact point P_w,

From equation 3.26:-

$$W_{pw} = W_{wR} + T_{wR}(C_{wR}{}^{P})$$

From equation 3.27:-

$$W_{wR} = 0i - yj + z\,k, \text{ where } z = f(y) = -\,0.025\,y - 42$$

$$W_{wR} = 0i - yj + (-\,0.025\,y - 42)k$$

From equation 3.39:-

$$T_{wR}(C_{wR}) = \begin{vmatrix} 0 & 0 & 0 \\ 0 & tjy^2(ni+nj+nk) & tj\, f(y)^2(ni+nj+nk) \\ 0 & tky^2(ni+nj+nk) & tk\, f(y)^2(ni+nj+nk) \end{vmatrix}$$

From Equation 3.35:-

$$t(y) = 0i + j - 0.025k$$

From equation 3.36:-

$$n(y) = 0i - 0.025\,j - k$$

From equation 3.30:-

$$f(y) = -\,0.025\,y - 42$$

And finally:-

$$ni + nj + nk = 0 - 0.025 - 1$$

$$= -1.025$$

Therefore the equation can be simplified as follows:-

$$T_{wR}(C_{wR}) = \begin{vmatrix} 0 & (0) & (0) \\ 0 & (1)(y^2)(-1.025) & (-\ 0.025\ y-42)^2(-1.025) \\ 0 & (-0.025)(y^2)(-1.025) & (-0.025)\ (-\ 0.025\ y-42)^2(-1.025) \end{vmatrix} \text{--(3.40)}$$

$$T_{wR}(C_{wR}) = \begin{vmatrix} 0 & 0 & 0 \\ 0 & (-1.025)(y^2) & (1.025)\ (0.025y+42)^2 \\ 0 & (0.026)(y^2) & (-0.026)\ (0.025y+42)^2 \end{vmatrix} \text{---------------- (3.41)}$$

Therefore the final equation for the ***right wheel*** become:-

$$\mathbf{W_{pR} = -yj - (0.025y+42)k +} \begin{vmatrix} \mathbf{0} & \mathbf{0} & \mathbf{0} \\ \mathbf{0} & \mathbf{(-1.025)(y^2)} & \mathbf{(1.025)\ (0.025y+42)^2} \\ \mathbf{0} & \mathbf{(0.026)(y^2)} & \mathbf{(-0.026)\ (0.025y+42)^2} \end{vmatrix} \text{---- (3.42)}$$

And for the ***left wheel*** the above equation will become:-

$$\mathbf{W_{pL} = yj + (0.025y+42)k +} \begin{vmatrix} \mathbf{0} & \mathbf{0} & \mathbf{0} \\ \mathbf{0} & \mathbf{(-0.975)(y^2)} & \mathbf{(-0.975)\ (0.025y+26)^2} \\ \mathbf{0} & \mathbf{(-0.0244)(y^2)} & \mathbf{(-0.0244)(0.334y+42)^2} \end{vmatrix} \textbf{---- (3.43)}$$

3.3 Wheel – Rail Contact Point Detection

From simple mathematics, in order to find the coordinate points of the contact point P the corresponding wheel and rail contact point equations has to equated, the result of this will give us candidates of the wheel rail contact point, P, coordinates. For instance to find the coordinates of contact points between the right rail and the right wheel equation 3.24 and 3.42 has to be equated.

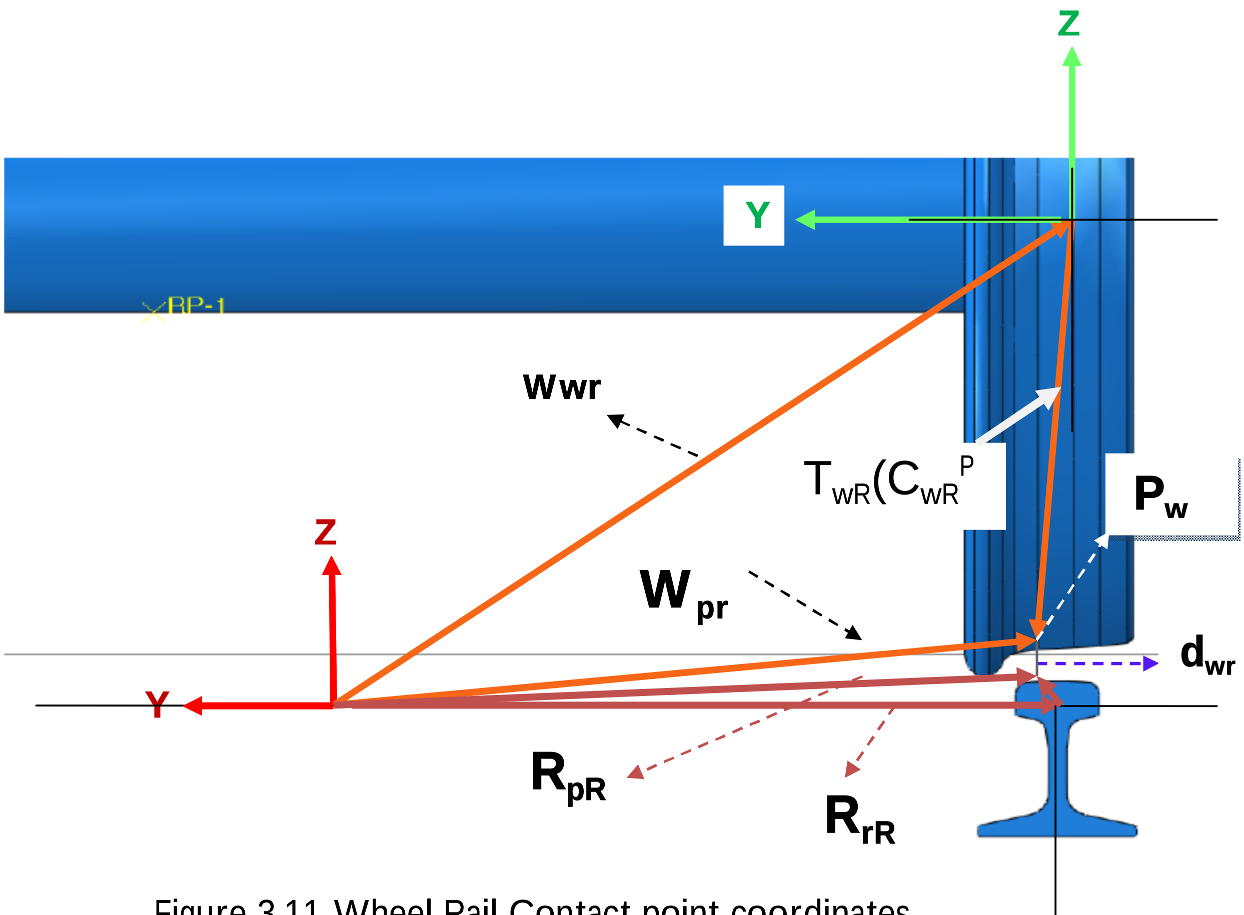

Figure 3.11 Wheel Rail Contact point coordinates.

From simple mathematics, in order to find the coordinate points of the contact point P the corresponding wheel and rail contact point equations has to equated, the result of this will give us candidates of the wheel rail contact point, P, coordinates. For instance to find the coordinates of contact points between the right rail and the right wheel equation 3.24 and 3.42 has to be equated.

$$\vec{R}_{pR} - \vec{W}_{PR} = d_{wr} \text{---} \quad (3.44)$$

Where:-

$\vec{\mathbf{R}}_{\mathbf{pR}}$= is a vector defining the position of the contact point P on the right rail from the global coordinate system.

$\vec{\mathbf{W}}_{\mathbf{PR}}$= is a vector defining the position of the contact point P on the right wheel from the global coordinate system.

$\mathbf{d}_{\mathbf{wr}}$= is the distance between the contact points on the rail and on the wheel.

From the figure 3.11 it is clear that in order to have a contact the distance between the contact points on the rail and the wheel have to be zero, $\mathbf{d}_{\mathbf{wr}}$=0.

Therefore,

$$\vec{\mathbf{R}}_{\mathbf{pR}} = \vec{\mathbf{W}}_{\mathbf{PR}} \text{--} \quad (3.45)$$

Where:-

$\vec{R}_{pR}=\vec{R}_{rR}+ T_{rR}(C_{rR}^{P})$,   and

$\vec{W}_{pr}=\vec{W}_{wR}+ T_{wR}(C_{wR}^{P})$

By assuming that $\vec{R}_{rR}$ and $\vec{W}_{pr}$ are zero, and then by substituting the components of the above equation from equation 3.24 for the rail, and 3.42 for the wheel, equation 3.45 will become:-

$$\begin{vmatrix} \mathbf{0} & \mathbf{0} & \mathbf{0} \\ \mathbf{0} & \mathbf{(-1.025)(y^2)} & \mathbf{(1.025)\ (0.025y+42)^2} \\ \mathbf{0} & \mathbf{(0.026)(y^2)} & \mathbf{(-0.026)\ (0.025y+42)^2} \end{vmatrix} =$$

$$\begin{vmatrix} \mathbf{0} & \mathbf{0} & \mathbf{0} \\ \mathbf{0} & \mathbf{(\frac{m}{30})(y^2)(-u+\frac{m}{30})} & \mathbf{(\frac{m}{30})(m-26.67)^2(-u+\frac{m}{30})} \\ \mathbf{0} & \mathbf{(u)(y^2)(-u+\frac{m}{30})} & \mathbf{(u)(m-26.67)^2(-u+\frac{m}{30})} \end{vmatrix} \text{-------------} \quad (3.46)$$

Where:-

$m = \sqrt{30^2 - y^2}$, and $u = \frac{y}{30}$.

From equation 3.46 there will be four alternative polynomial equations. All of these equations will yield different candidate coordinates for the contact point P.

Equation 1:-

$$\mathbf{(-1.025)(y^2) = (\frac{m}{30})(y^2)(-u+\frac{m}{30})}$$

Equation 2:-

$$\mathbf{(1.025)\ (0.025y+42)^2 = (\frac{m}{30})(m-26.67)^2(-u+\frac{m}{30})}$$

Equation 3:-

$$\mathbf{(u)(y^2)(-u+\frac{m}{30}) = (u)(y^2)(-u+\frac{m}{30})}$$

Equation 4:-

$$\mathbf{(-0.026)\ (0.025y+42)^2 = (u)(m-26.67)^2(-u+\frac{m}{30})}$$

Consequently, the corresponding solutions for contact point coordinates are:-

Solution for equation1 (cm):-

(X, Y, Z) = (0, 0, 3.33),

Solution for equation 2 (cm):-

(X, Y, Z) = (0, 8.464, 2.111),

Solution for equation 3:-

(X, Y, Z) = (0, 0, 3.33),

Solution for equation4:-

(X, Y, Z) = (0, 1.4484, 3.2950).

N.B –The above solutions are measured from the right rail local coordinate axis.

Among the above solutions there are only two possible solutions, i.e. P_1 = (0, 0, 3.33) and P_2= (0, 1.4484, 3.2950). However, when the wheel and the rail are assembled in ABAQUS based on $P_{1,}$ the left wheel will not have the same contact coordinate point with the right wheel. Therefore, the valid coordinates for contact point P between the right rail and right wheel will be P_2= (0, 1.4484, 3.2950).

4 - DETERMINATION OF CONTACT AREA

4.1 Hertzian Contact Area Calculation

As it is stated under section 1.3.2.2 Hertzian contact theory will be followed for the calculation of contact stress. Therefore, according to Hertz theory, the normal pressure is distributed as an ellipsoid over the elliptic contact area with semi-axes a and b.

The ellipsoidal contact pressure distribution $P(x, y)$ is expressed by:-

$$P(x, y) = \frac{3F_n}{2\pi ab}\sqrt{1 - \left(\frac{x}{a}\right)^2 - \left(\frac{y}{b}\right)^2},$$

When x and y values are zero, i.e. at the center of the ellipse, the contact pressure will be maximum. The maximum pressure P_o is :-

$$P_o = \frac{3F_n}{2\pi ab} \text{--} (4.1)$$

According to [8] the semi axes of the ellipse a and b are:-

$$a = e\left[\frac{3\pi\ F_n(Kr+Kw)}{4\ (A+B)}\right]^{1/3} \text{----------------------------------} (4.2)$$

$$b = n\left[\frac{3\pi\ F_n(Kr+Kw)}{4\ (A+B)}\right]^{1/3} \text{-------------------------------------} (4.3)$$

Where,

a = semi axis in the x direction.

b= semi axis in the y direction.

e & n = semi axis coefficients.

$K_r = \frac{(1-\grave{\upsilon}_r)}{\pi\ Er}$ and

$K_w = \frac{(1-\grave{\upsilon}_w)}{\pi\ Ew}$,

Where:-

$\grave{\upsilon}_r$ = poison's ratio for the rail

$\grave{\upsilon}_w$ = poison's ratio for the wheel

E_r = young's modules for the rail and wheel.

E_w = young's modules for the wheel.

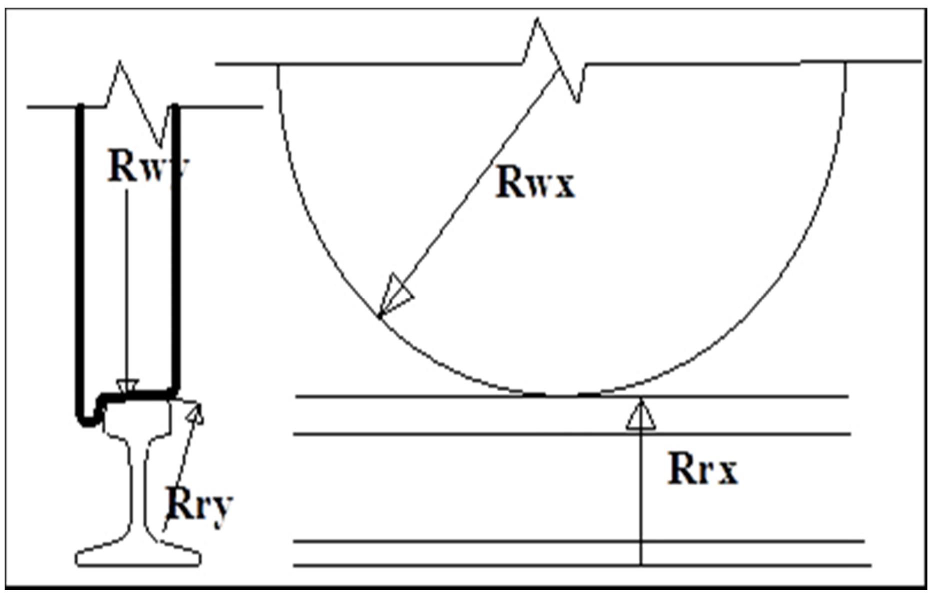

Figure 4.1 Wheel and Rail Principal Radii

From [8] the components of equation 4.2 and 4.3 can be written as follows:-

$$A + B = \frac{1}{2}\left(\frac{1}{Rrx} + \frac{1}{Rry} + \frac{1}{Rwx} + \frac{1}{Rwy}\right) \text{---------------------} \quad (4.4)$$

$$B - A = \frac{1}{2}\left[\left(\frac{1}{Rwx} - \frac{1}{Rwy}\right)^2 + \left(\frac{1}{Rry} - \frac{1}{Rrx}\right)^2 + 2\left(\frac{1}{Rwx} - \frac{1}{Rwy}\right)\left(\frac{1}{Rrx} - \frac{1}{Rry}\right)\cos 2\varphi\right]$$

Where:-

φ=The angle between the principal planes, in our case φ =0^0 for straight track.

Therefore, B-A becomes:-

$$B–A=\frac{1}{2}\left[\left(\frac{1}{Rwx}-\frac{1}{Rwy}\right)^2+\left(\frac{1}{Rry}-\frac{1}{Rrx}\right)^2+2\left(\frac{1}{Rwx}-\frac{1}{Rwy}\right)\left(\frac{1}{Rrx}-\frac{1}{Rry}\right)\frac{1}{1}\right]..(4.5)$$

Also from [8] the semi axes coefficients m and n can be written as follows:-

e= 62.19($\theta^{-0.914}$)-- (4.6)

n= (3 x 10^{-5})(θ^2) + 0.0045 θ+ 0.334 ------------------------------- (4.7)

Where $\theta = \cos^{-1}\frac{B-A}{A+B}$--- (4.8)

In this thesis 25 ton of axle load will be used, this leads to 125 KN normal force on the right and left wheel and the two bodies that are in contact are assumed to have identical material properties with Young's modulus 200GPa and Poisson's ratio 0.3.
This follows:-

F_n = 125 KN, and

R_{rx}= ∞ , R_{ry} = 0.3m

R_{wx} = 0.42m, R_{wy} = ∞

$\grave{\upsilon}_r$ and $\grave{\upsilon}_w$ = 0.3

E_r = E_w= 200GPa

Therefore,

$$A + B =\frac{1}{2}\left(\frac{1}{\infty}+\frac{1}{0.3}+\frac{1}{0.42}+\frac{1}{\infty}\right)$$

$A + B = 2.860$

$$B–A=\frac{1}{2}\left[\left(\frac{1}{Rwx}-\frac{1}{Rwy}\right)^2+\left(\frac{1}{Rry}-\frac{1}{Rrx}\right)^2+2\left(\frac{1}{Rwx}-\frac{1}{Rwy}\right)\left(\frac{1}{Rrx}-\frac{1}{Rry}\right)\frac{1}{1}\right]$$

$$B–A=\frac{1}{2}\left[\left(\frac{1}{0.42}-\frac{1}{\infty}\right)^2+\left(\frac{1}{0.3}-\frac{1}{\infty}\right)^2+2\left(\frac{1}{0.42}-\frac{1}{\infty}\right)\left(\frac{1}{\infty}-\frac{1}{0.3}\right)\frac{1}{1}\right]^{1/2}$$

$B – A = 0.476$

$\cos\theta = \frac{B-A}{A+B}$

$\cos\theta = 0.167$

$\theta = \cos^{-1}(0.167)$

$\theta = 80.41^0$

From equation 4.6 and 4.7 the value of m and n becomes:-

$e=62.19\ (80.41^{-0.914})$

$e = 1.128$

$n= (3 \times 10^{-5})(80.41^2) + (0.0045 \times 80.41) + (0.334)$

$n = 0.890$

and, K_r and K_w will become:-

$K_r = \frac{(1-0.3)}{\pi\ (200GPa)}$

$= 1.11 \times 10^{-12}/Pa$

$K_w = \frac{(1-0.3)}{\pi\ (200GPa)}$

$= 1.11 \times 10^{-12}\ /Pa$

Therefore, the semi axes for the ellipsoid contact area will become:-

$$a = e\left[\frac{3\pi\ F_n(Kr+Kw)}{4\ (A+B)}\right]^{1/3} \text{----------------------------------} \quad (4.9)$$

$$= 1.122\left[\frac{3\pi\ (125KN)(2*1.11\ E-9/KPa)}{4\ (2.860)}\right]^{1/3}$$

***a* = 0.00691 m**

$$b = n\left[\frac{3\pi\ F_n(Kr+Kw)}{4\ (A+B)}\right]^{1/3}$$

$$= 0.894\left[\frac{3\pi\ (125KN)(2*1.11\ E-9/KPa)}{4\ (2.860)}\right]^{1/3}$$

***b* = 0.00545 m**

Accordingly, the ellipsoid contact area becomes:-

Area = π x *a x b*

***A*= 1.183 x 10^{-4} m^2**

***A*= 118.3 mm^2**

5. FINITE ELEMENT MODELING AND SIMULATION

5.1 Detailed Modeling Procedure

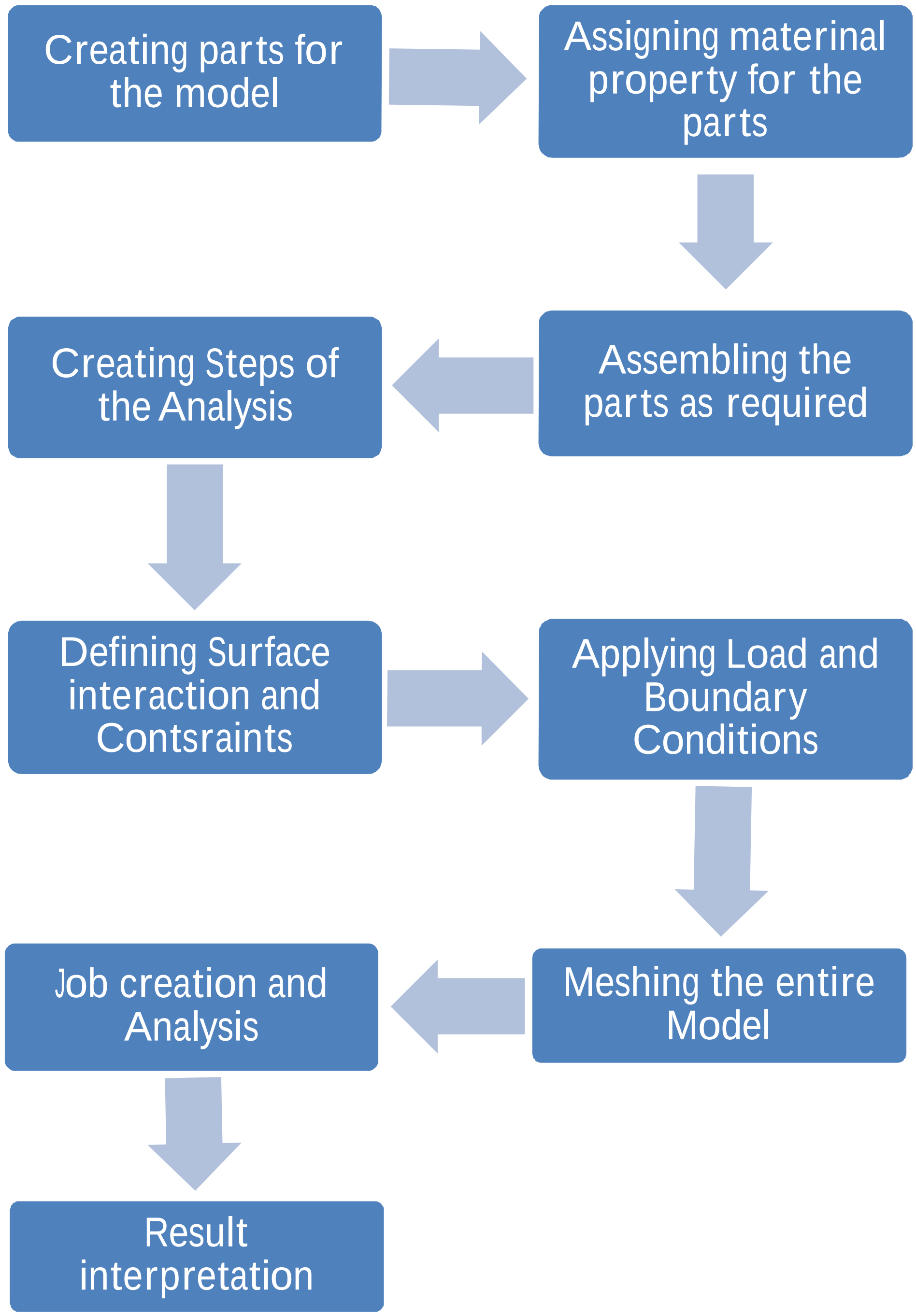

Figure 5.1 Modeling procedure

Parts are the building blocks of an ABAQUS model, therefore creating them is the first step to the simulation process. In this thesis there are two parts involved, the rail and the wheel, first the rail part will be created all the other cross sectional dimensions are taken from [6].

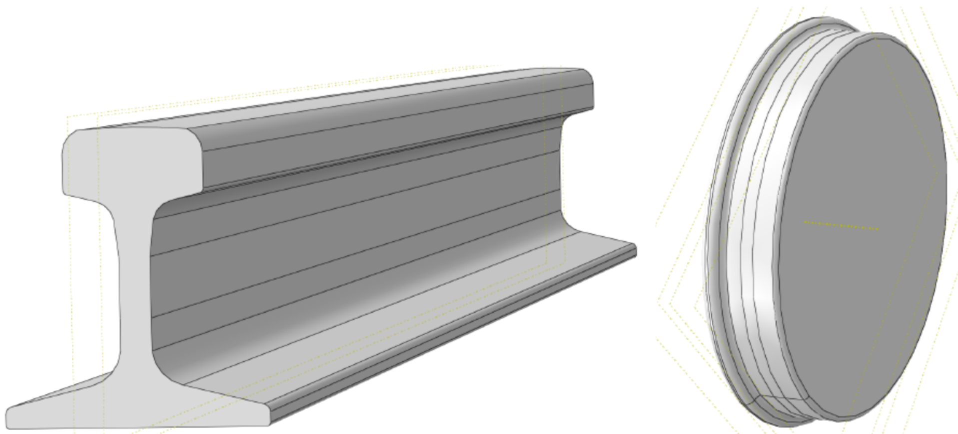

Figure 5.2 Rail and wheel Part

The next step is assigning the material property for the created parts and the material definition specifies all the property data relevant to a material. The material definition is specified by including a set of material behaviors such as density, modulus of elasticity, and poisons ratio. Accordingly, solid and homogeneous section category is selected for both the rail and the wheel parts. In the following table all the parameters used are listed.

Table 5.1 Modeling parameters

No.	Used Parameter	Unit	Value
1	Wheel modulus of Elasticity (Er)	GPa	200
2	Wheel modulus of Elasticity (Ew)	GPa	200
3	Wheel material density	Kg/m^3	7850
4	Rail material density	Kg/m^3	7850
5	Poison's ratio	Non	0.3
6	Wheel radius	m	0.42
7	Applied wheel load	kN	125
8	Wheel meshing dimension	mm	10
9	Rail meshing dimension	mm	10

Our model contains one main assembly which is composed of instances of parts from the model. In order to minimize cost of the analysis the assembly will only involve the right wheel and the right rail. Moreover, for the analysis and result comparison purpose there will be two categories of main assembly; i.e. with and without track irregularities.

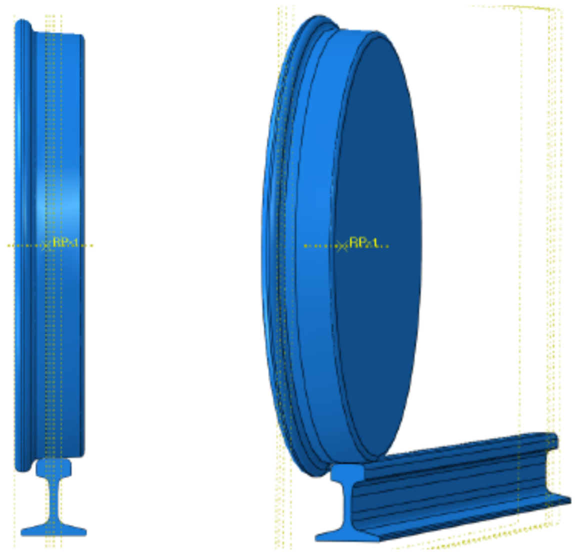

Figure 5.3 Wheel and Rail assembly

Assembled model for simulation of wheel rail contact without track irregularity will follow the coordinates for the contact point P found in section 3.3. However, Simulation for tracks with irregularities will be done by adjusting the wheel according to the applied irregularities, for instance in order to model +30mm alignment irregularity, the y coordinate of the previous contact point P, without irregularity, will be changed to $y_2 = y_1 + 30mm$, where y_1 is y coordinate for point P without irregularity and y_2 is the new y coordinate for the +30mm alignment irregularity. Accordingly, for the vertical or longitudinal irregularity the z coordinate will be adjusted.

Within the model a sequence of two analysis step is defined. These step sequences provide a convenient way to capture changes in the loading and boundary conditions of the model. Specifically the first step is used to load a 125kN on the center of the wheel with a time period of 0.1sec and the second step is used to move the wheel on the rail with a time period of 1sec. both steps follow a static, general analysis type.

The next step is defining the interaction property and constraints. Generally, interaction is a step dependent object. For modeling under this paper surface-to-surface contact interaction is used and it will define contact between the deformable, the rail, and rigid, wheel, surfaces. Afterwards, constraints have to be defined on the analysis degrees of freedom. A coupling constraint is used in this modeling section and it constrains the motion of the surface of the wheel to the motion of a single point, i.e. the wheel center.

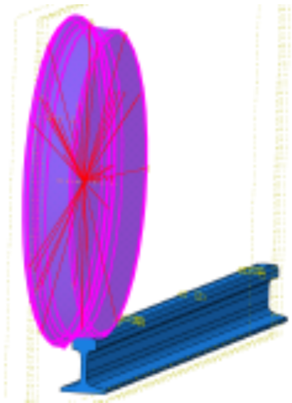

Figure 5.4 Interaction and constraints

After determining the analysis steps of the model loading module definition will be followed. Since a 25ton track is assumed for the simulation each wheel will receive 125kN load from the axle. Accordingly, this load is applied as a concentrated force on the center of the wheel pointing downward. In addition, the rail bottom surface will be given a fixed boundary condition.

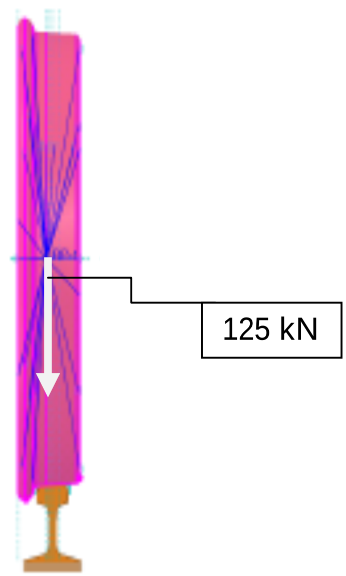

Figure 5.5 Loading the Assembly

In order to conduct a finite element analysis meshes with appropriate dimension will be generated on the created parts.

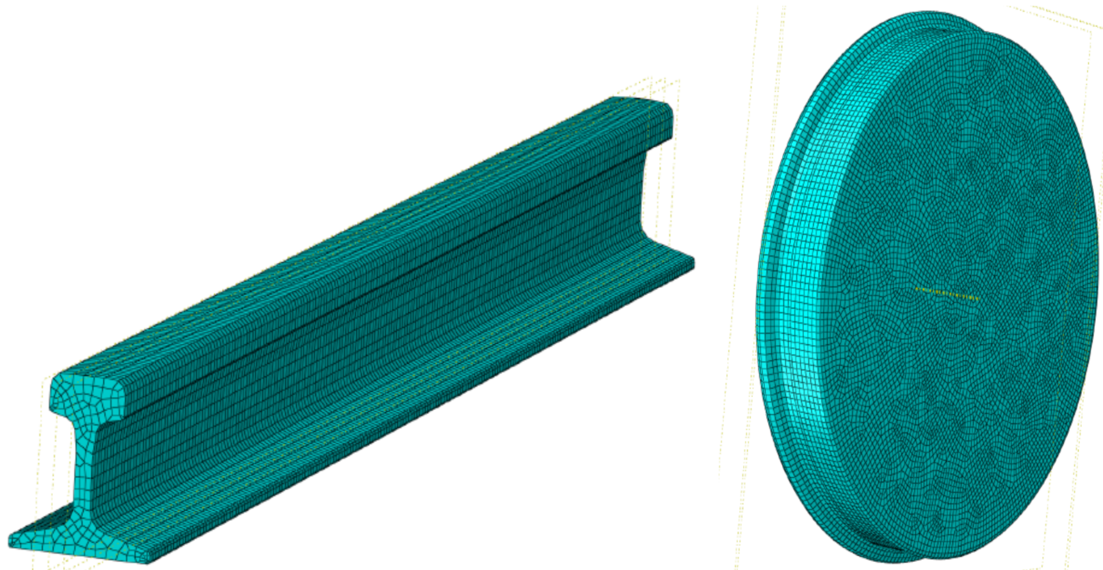

Figure 5.6 wheel and rail meshing

Finally, after finishing all of the tasks involved in defining the model the last step is to create a job and submit it for analysis.

6. RESULTS AND DISCUSSION

6.1 General

Based on the procedure illustrated in section 5.2 two categories of simulations will be done, with and without track irregularities. For tracks without track irregularity there will be only one model and for tracks with irregularities we will have generally two models one for alignment/gauge irregularity and another for longitudinal/cross level irregularity. Furthermore, there will be four sub-models for each irregular model.

Table 6.1 Model description

Model Without Irregularity	Model With Irregularity	
	Lateral Irregularity (Alignment/Gauge)	**Vertical Irregularity (Longitudinal/Cross Level)**
Model 1= On point P*	**Model 2 =** Shifting the right wheel -8mm laterally= -8mm	**Model 6 =** Moving the right rail 10mm upward = +10mm**
N/A	**Model 3 =** Shifting the right wheel 10mm laterally= +10mm	**Model 7 =** Moving the right rail 20mm upward = +20mm**
N/A	**Model 4 =** Shifting the right wheel 20mm laterally= +20mm	**Model 8 =** Moving the right rail 30mm upward = +30mm**
N/A	**Model 5 =** Shifting the right wheel 30mm laterally= +30mm	N/A

N.B:-

***** Coordinate for point P is from section 3.2 which is = (0, 1.4484, 3.29502).

****** When we move the right rail upward the corresponding right wheel will be tilted counterclockwise.

6.2 <u>Results for Tracks without irregularity</u>

In this section the variation of the wheel-rail contact geometry, contact pressure and normal contact forces with and without the presence of the applied track irregularities for all the models described in table 6.1 will be shown with the help of graphs and contour plots.

<u>Typical Wheel Rail Contact Geometry</u>

According to Hertzian contact theory the geometry of the wheel rail contact is assumed to be elliptic contact patch, it is clearly shown in the simulation result, figure 6.1 that the geometry of the contact area between the rail and the wheel is approximately an elliptic area.

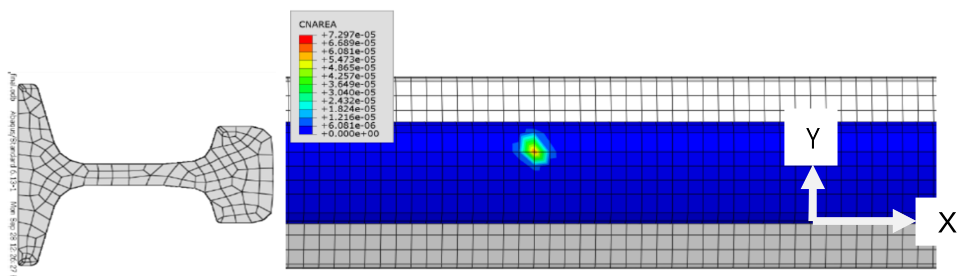

Figure 6.1 Contact area geometry & location (right rail)

The magnitude of the contact area at the contact node is 6.40E-05 m^2 and the contour plot for the contact area is shown in figure 6.2 below.

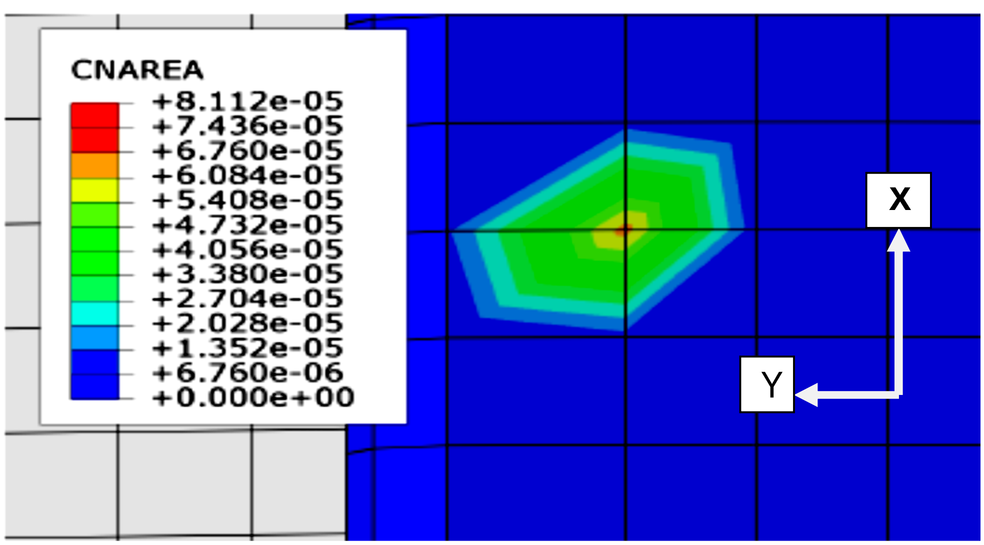

Figure 6.2 Contact area contour for right rail (m^2)

Normal Contact force and pressure

According to Hertz theory, the normal contact pressure is distributed as an ellipsoid over the elliptic contact patch and the maximum contact pressure occurs at the center of the contact patch. The longitudinal and transversal projection of the contact pressure distribution is given as follows.

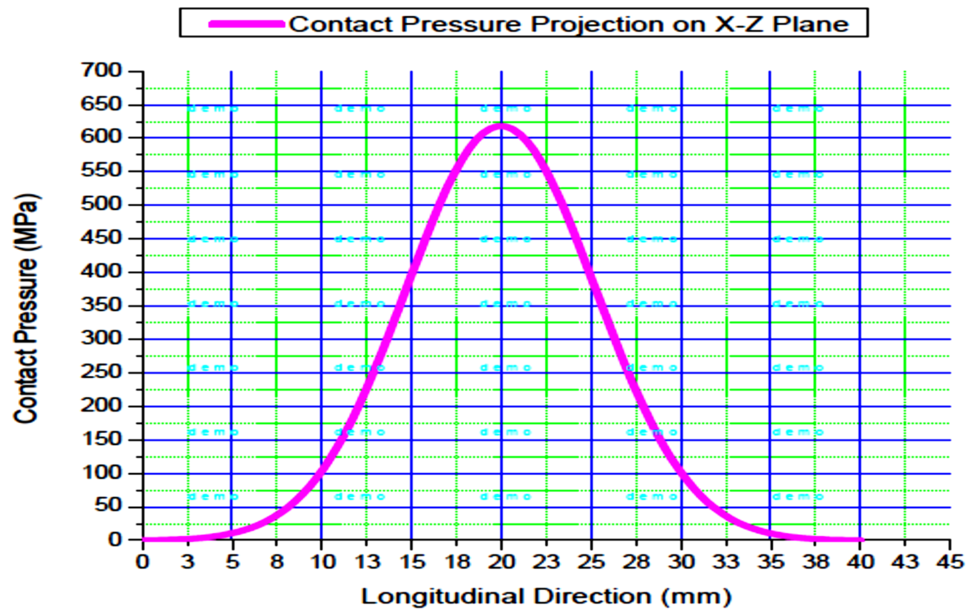

Figure 6.3 Longitudinal projection of the contact pressure.

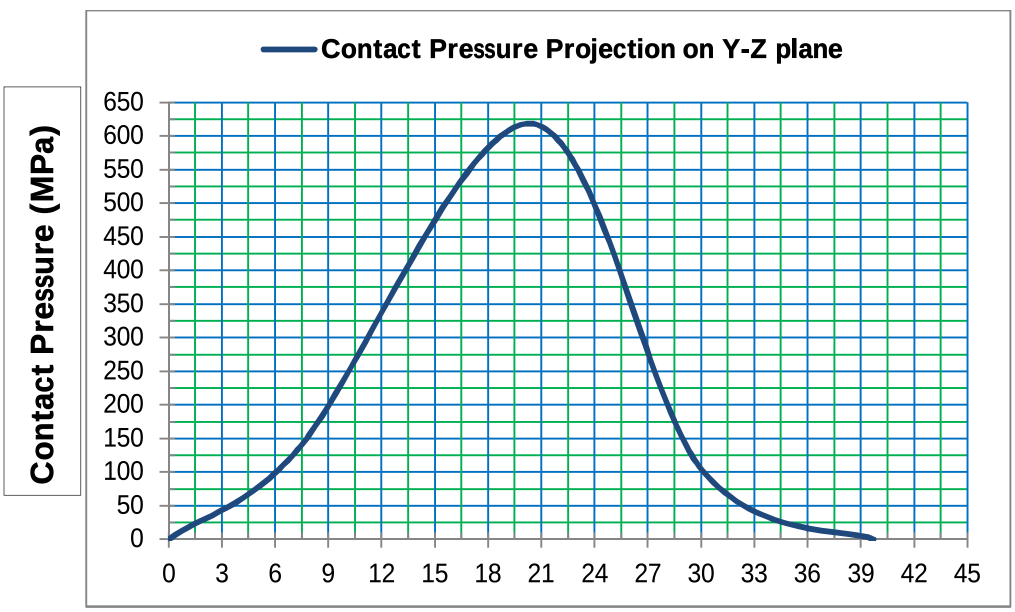

Figure 6.4 Transversal projection of the contact pressure.

The maximum contact pressure for the simulated result is 618.34 MPa and also as shown in the figure below the contact pressure distribution follows an ellipsoid distribution.

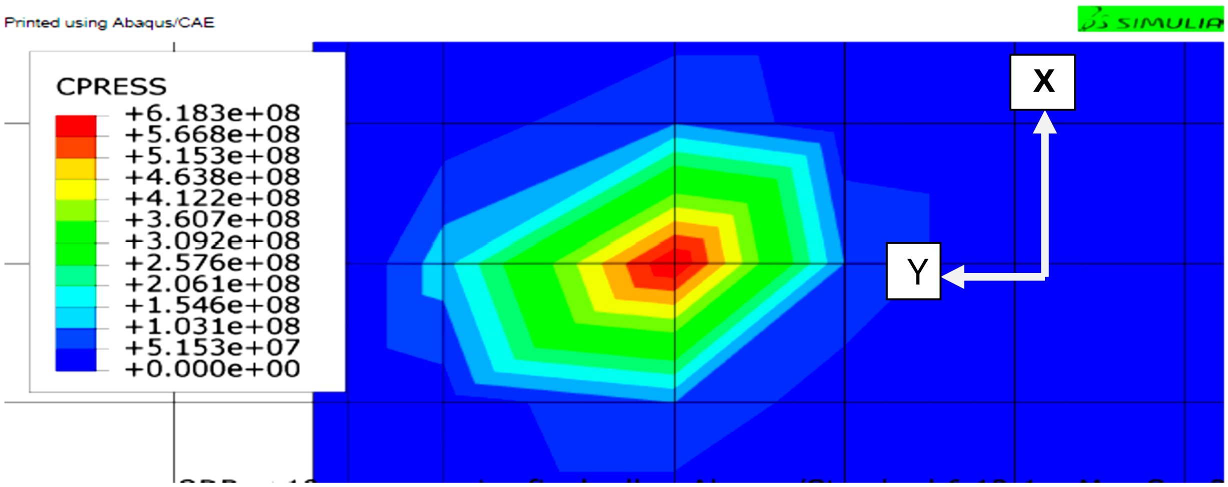

Figure 6.5 Contact patch colored contour plot for the right rail (Pa)

Moreover, the maximum normal contact nodal force is 70.414 kN which is acting at the center of wheel rail contact patch.

6.3 Results for Alignment/gauge Track irregularity

Wheel Rail Contact Geometry

In order to see the effect of alignment/gauge irregularity on the wheel rail contact geometry, four simulation models are applied, -8mm, +10mm, +20mm, and +30mm lateral shifting of the right wheel. According to the result drawn from ABAQUS 6.13.1the location for the contact patch are situated in the figure 6.6 below.

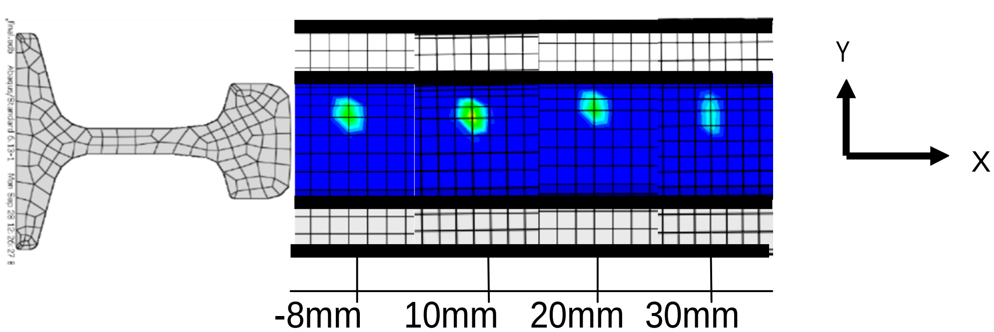

Figure 6.6 Alignment/Gauge irregularities Vs Contact patch location.

The magnitude of the contact area at the contact node varies in accordance with the applied irregularity as follows.

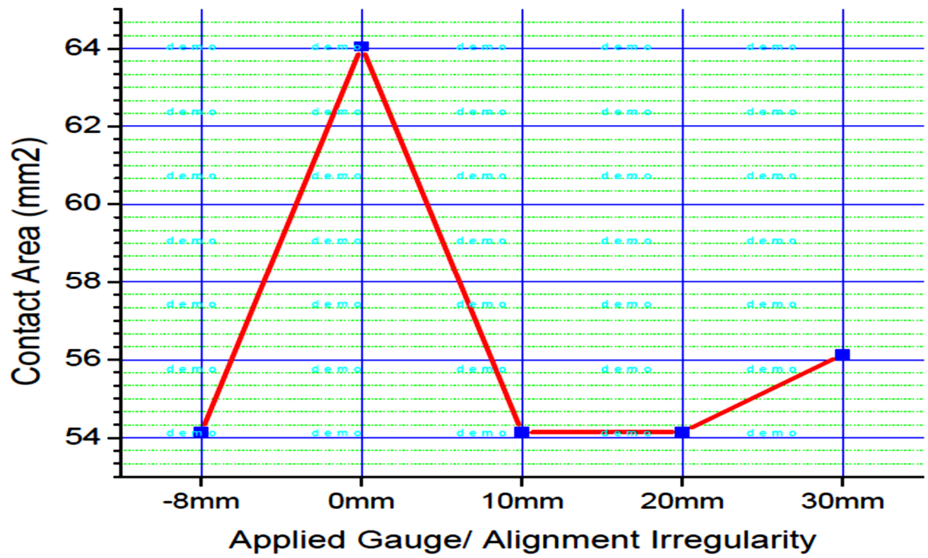

Figure 6.7 Contact area magnitude difference with alignment/gauge irregularity

Normal Contact Force and Pressure

The magnitude of the Normal contact force and Pressure at the contact node varies in accordance with the applied irregularity as follows.

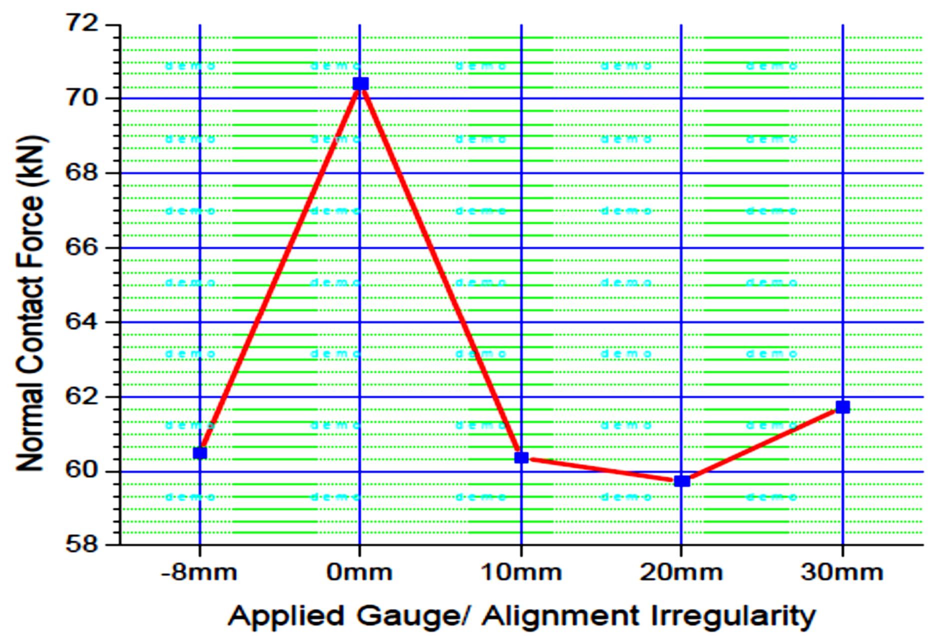

Figure 6.8 Normal Contact Force Vs applied alignment/gauge irregularity

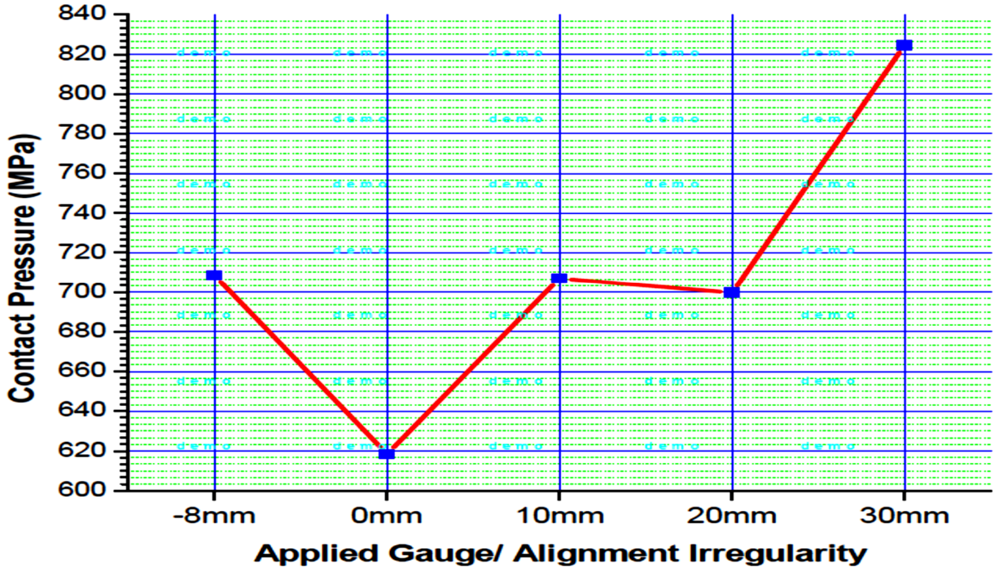

Figure 6.9 Normal Contact pressure Vs applied alignment/gauge irregularity

6.4 Results for Longitudinal/Cross Level Track irregularity

Wheel Rail Contact Geometry

Keeping in mind that this thesis paper is based on the Hertz contact theory, i.e. there will only be one contact point between the rail and the wheel, three simulation models are applied, +10mm, +20mm, and +30mm upward shifting of the right wheel and rail this is in order to see the effect of Longitudinal/cross level irregularity on the wheel rail contact geometry. However, it is impossible to simulate +40mm upward longitudinal/cross level irregularity this is because there will be a two point contact. According to the result drawn from ABAQUS 6.13.1the location for the contact patch are situated in the figure below.

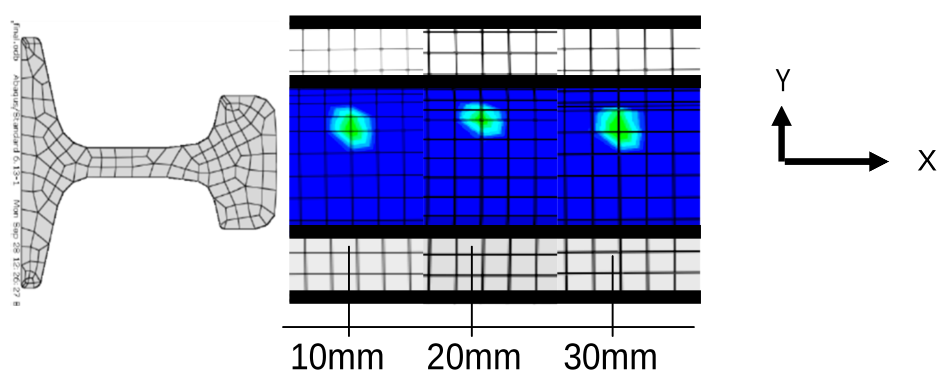

Figure 6.10 Longitudinal/Cross level irregularities Vs Contact patch location.

The magnitude of the contact area at the contact node varies in accordance with the applied irregularity as follows.

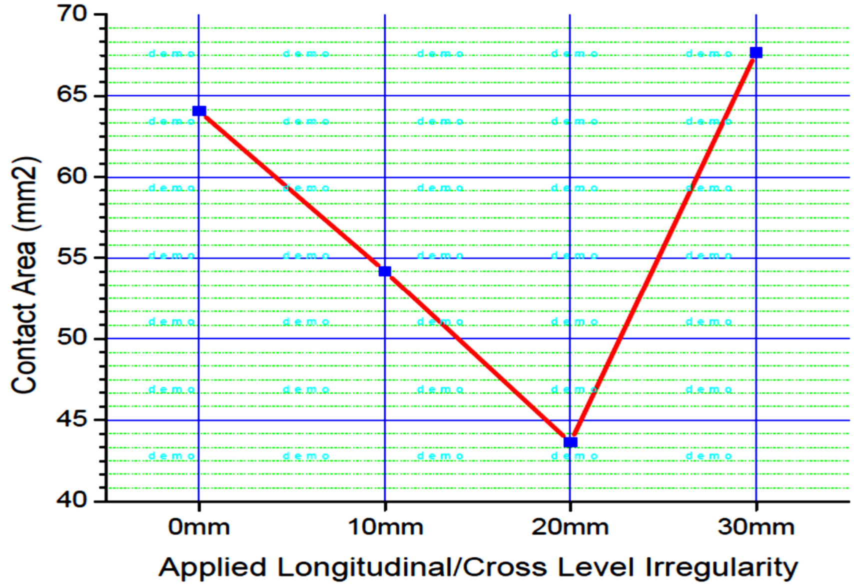

Figure 6.11 Contact area Vs applied Longitudinal/ Cross level irregularity

Normal Contact Force and Pressure

The magnitude of the Normal contact force and Pressure at the contact node varies in accordance with the applied irregularity is as follows.

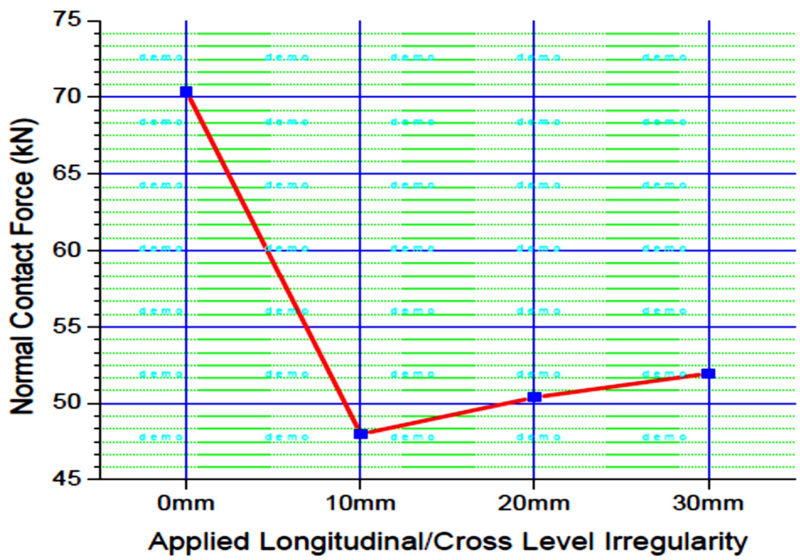

Figure 6.12 Normal Contact Force Vs applied Longitudinal/Cross level irregularity

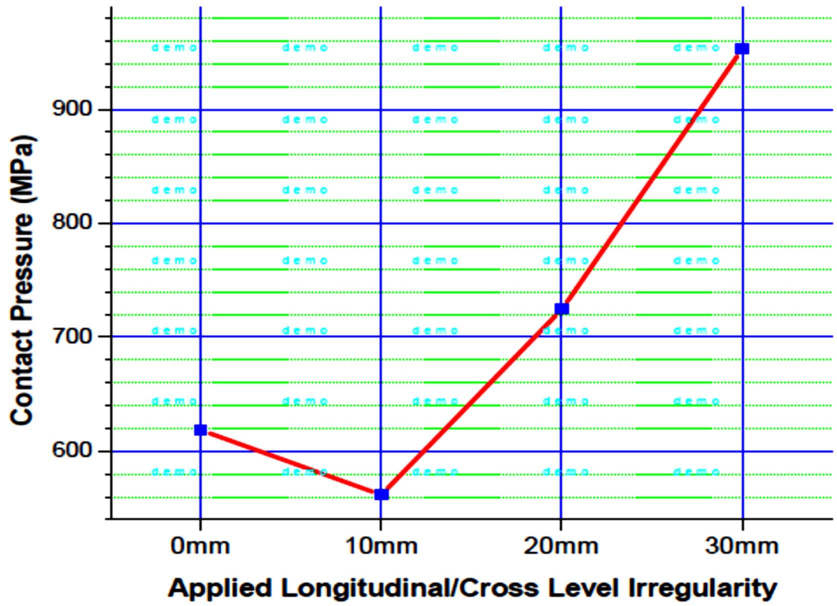

Figure 6.13 Normal Contact Pressure Vs applied Longitudinal/Cross level irregularity

Table 6.2 ABAQUS result summary.

Types of Applied Irregularity	Applied Magnitude	**Contact Pressure (MPa)**	**Contact Area (mm^2)**	**Normal Contact Force (kN)**
No Irregularity	0mm	618.333	64.048	70.4142
Longitudinal /Cross Level	10mm	561.768	54.176	47.9821
	20mm	724.367	43.620	50.3983
	30mm	953.101	67.655	51.9529
Alignment /Gauge	-8mm	708.529	54.141	60.488
	10mm	706.954	54.142	60.3538
	20mm	699.654	54.144	59.7321
	30mm	824.503	56.134	61.7205

7. CONCLUSION AND RECOMMENDATION

7.1 Conclusion

From the analysis of wheel and rail surface geometry the contact point is computed mathematically based on Hertz contact theory and identified as a point contact. Therefore, the coordinates for the contact point for the right rail and right wheel is computed as P = (0, 1.4484, 3.2950), note that this coordinate is measured from the simplified coordinate system as shown in figure 3.3.

After the wheel-rail contact point is identified Hertzian contact theory is applied to calculate the contact area, section 4.1. Accordingly, for an applied normal wheel load of 125kN, the contact area was found to be 118.3 mm^2. In addition to this, there are eight ABAQUS models which are used to simulate a point contact between the rail and the wheel, four for the lateral irregularities, three for the vertical irregularities and one model in order to simulate tracks without irregularity.

The magnitudes of the applied irregularities are taken from table 2.4, and among the three quality levels stated in section 2.3.2 the alert and intervention limit values are used. This is because alert and intervention limit values are mainly linked with maintenance policy. Moreover, if a limit value is exceeded at this level, an action that corrects the error has to be done before the next inspection, i.e. maintenance, speed restrictions [4].

As we can see from table 6.2 there is an increase in the contact pressure and the contact area when the applied irregularity is increasing, both for lateral and vertical irregularity. For instance, for +30mm vertical and lateral irregularity the contact pressure became 953.101 MPa and 824.503 MPa respectively, and also the contact area became 67.655m^2 and 56.134m^2 respectively. However, the normal contact force resulted from ABAQUS is maximum when there is no irregularity, which is 70.414 kN, and among the models with irregularity the normal contact force is maximum when the applied irregularity is maximum.

Table 6.3 shows the corresponding changes in the three parameters, i.e. contact pressure, contact area and normal contact force, with the applied vertical and lateral irregularities as compared to the results from model #1, model without irregularity.

Table 6.3 Recorded changes with respect to Model #1.

Types of Applied Irregularity	Applied Magnitude	Changes with respect to Model # 1		
		Con. Press. (MPa)	Con. Area (mm^2)	Normal Con. Force (kN)
Vertical Irregularity	10mm	**-9.15%**	**-15.41%**	**-31.86%**
	20mm	**17.15%**	**-31.89%**	**-28.43%**
	30mm	**54.14%**	**5.63%**	**-26.22%**
Lateral Irregularity	-8mm	**14.59%**	**-15.47%**	**-14.10%**
	10mm	**14.33%**	**-15.47%**	**-14.29%**
	20mm	**13.15%**	**-15.46%**	**-15.17%**
	30mm	**33.34%**	**-12.36%**	**-12.35%**

7.2 Recommendation and future work

Based on the analysis results, the following recommendations are drawn:-

- Due to the applied +30mm vertical and lateral irregularity the contact pressure increases by 54.14% and 33.35%, respectively. Thus much emphasis should be given to avoid these irregularities.
- During the simulation process it is observed that more than +30mm and less than -8mm irregularity cannot be simulated to satisfy a one point contact scenario, modeling these will induce a two point contact scenario, one point on the rail head and the other contact point on the gauge corner of the rail.
- Due to the application of finite element model the numerical solutions differ significantly from the Hertzian solution, thereby the maximum contact pressure is overestimated by the Hertzian theory.

Since this thesis is based on Hertz contact theory; the effect of both lateral and vertical irregularities needs to be studied for the two point contact mechanism and also investigation of the above effects on the maintenance policy and safety procedures has to be conducted in the future works.

References:

[1] K.L. Johnson, Contact Mechanics, Cambridge University Press, Cambridge, UK, 1985.

[2] N. Zong, M. Dhanaseker, "Analysis of Rail Ends under Wheel Contact Loading", International Journal of Mechanical and Aerospace Engineering,6, 2012, pp. 452-460.

[3] British standard, "Railway Applications - track - track geometry quality - part 1: characterization of track geometry, EN 13848-1", British Standard institution, 2003".

[4] British standard, "Railway Applications-track-track geometry quality-part 5- geometric quality levels- plain line, BS EN 13848-5", British Standard institution, 2008.

[5] Jao Pombo, Jorge Ambrosio, and Miguel Silva, A new wheel rail contact model for railway dynamics, Instituto Superior Tecnico, Lisbon, Portugal, 2005.

[6] National Standards of the People's Republic of China, Hot-rolled steel rails for railway, GB 2585 – 2007.

[8] Jay Prakash Srivastava, P.K. Sarkar, and Vinayak Ranjan, "An Approximate Analysis for Hertzian Elliptic Wheel-Rail Contact Problem", Department of Mechanical Engineering, Indian School of Mines, Dhanbad, India, 2013.

[9] Sabine Damme, Udo Nackenhorst, Anja Wetzel, and Bernd W. Zastrau, "On the Numerical Analysis of the Wheel-Rail System in Rolling Contact", Lehrstuhl fur Mechanik, Technische Universitat Dresden, and Institut fur Baumechanik und Numerische Mechanik, Universitat Hannover

[10] Kenneth P. Kramp, "The Analysis and Creation of Track Irregularities Using TRAKVU", Virginia Polytechnic Institute and State University, Blacksburg, Virginia, 1998.

[11] V.A. Profillidis, "Railway Engineering", Section of Transportation, Democritus Thrace University, Greece, 1995.

[12] Prof. Elias Kassa, "Railway Engineering Design I –CENG 6902 Lecture note", Addis Ababa Institute of Technology, Addis Ababa, Ethiopia, 2013.

[13] Government of India Ministry of Railways (Railway Board), "Indian Railways Permanent Way Manual", New Delhi, India, 2004.

[14] K. Tomas, Track Irregularities for high- speed Trains, KTH Engineering Science, Stockholm, Sweden, 2009.

Annex: A

Tracks with Alignment/Gauge irregularity

-8mm Applied Irregularity

Wheel Rail Contact Geometry

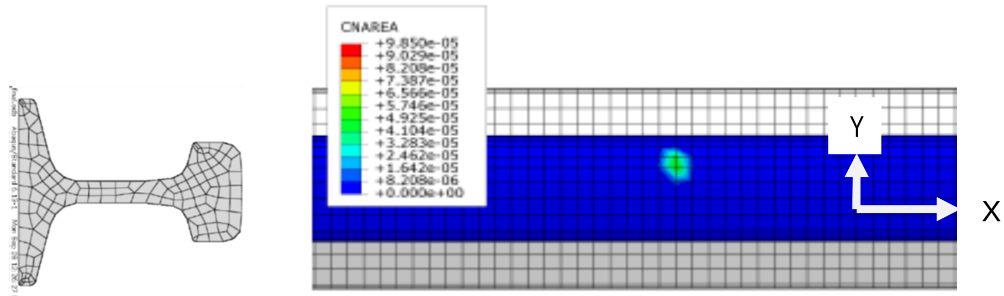

Figure A-1 Contact area geometry & location (right rail)

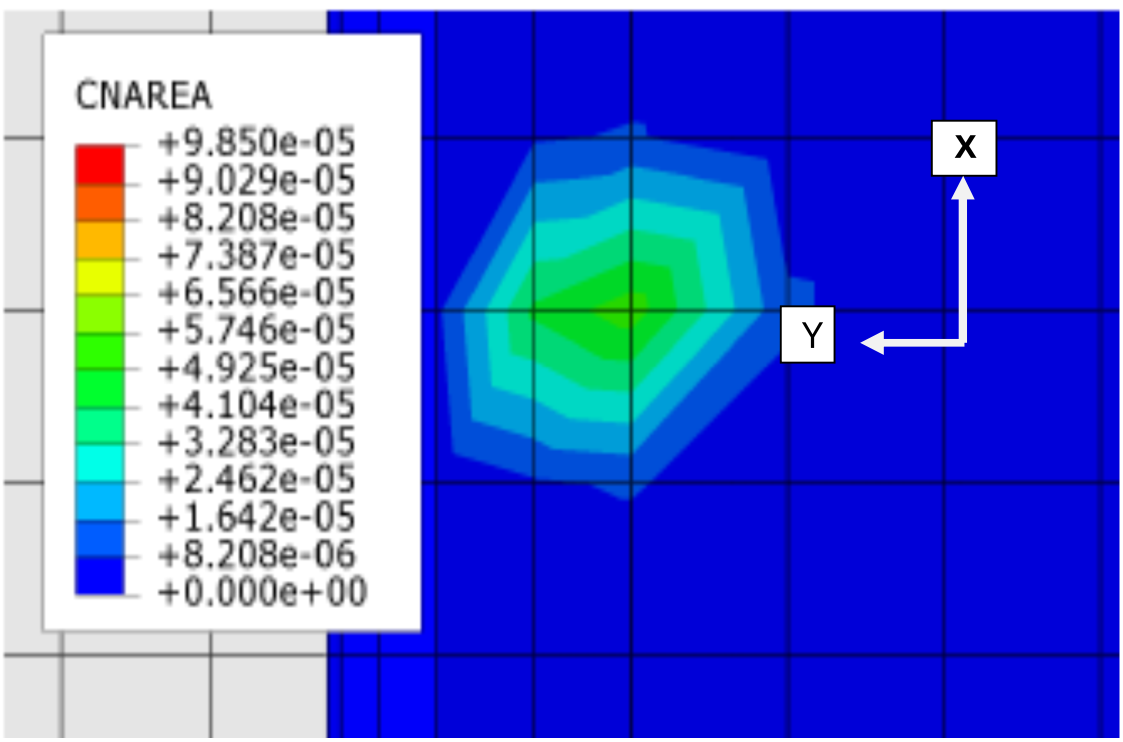

Figure A-2 Contact area contour for right rail (m^2)

Normal Contact pressure (-8mm applied lateral irregularity for right rail)

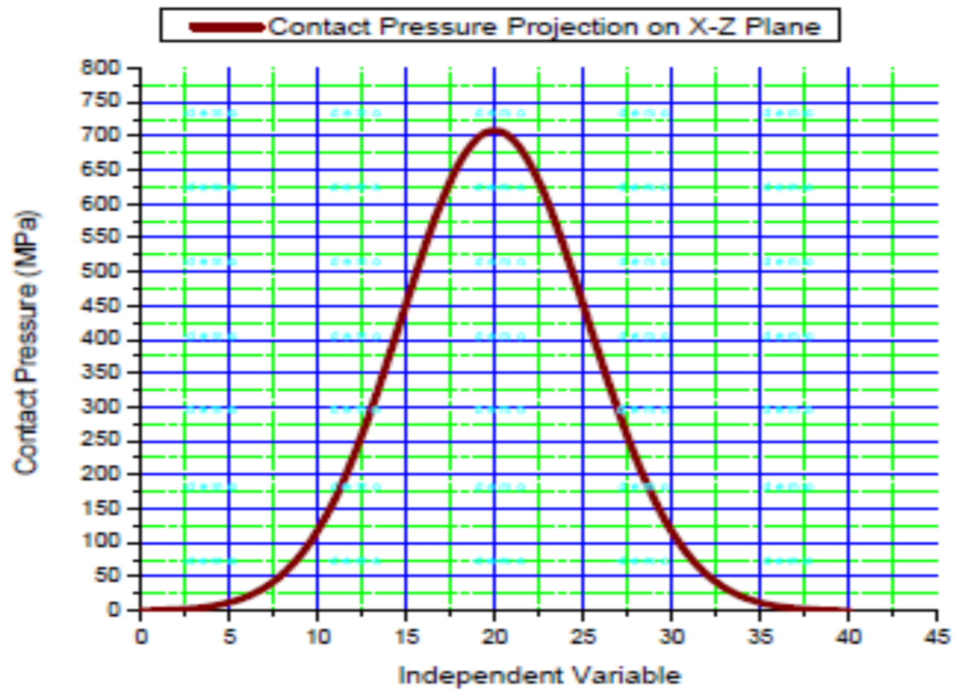

Figure A-3. Contact pressure projection on X-Z plane.

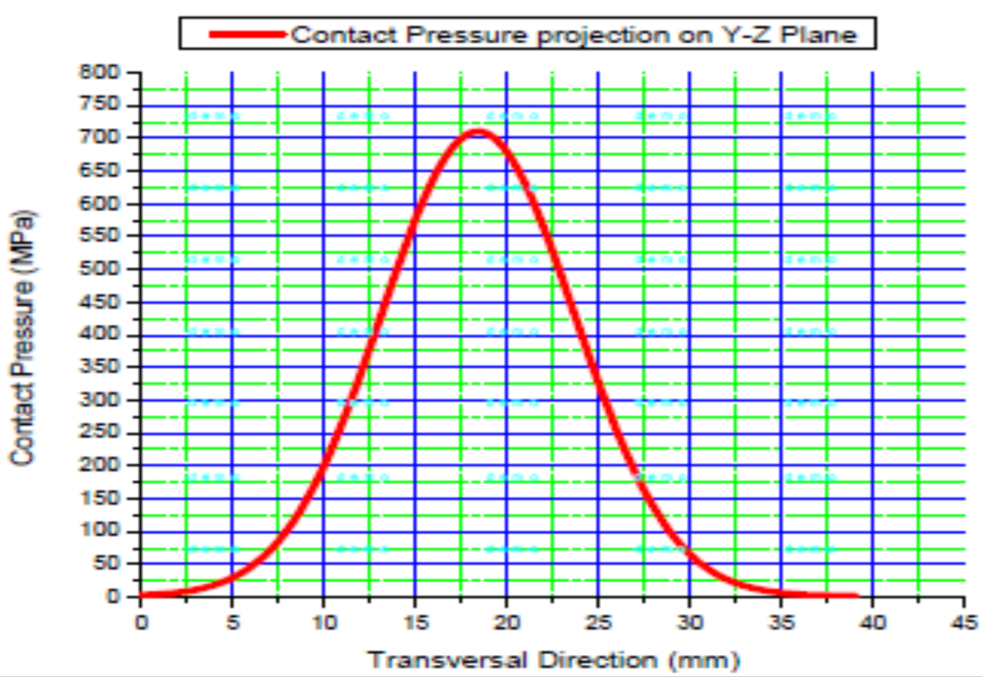

Figure A-4. Contact pressure projection on Y-Z plane.

30mm Applied Irregularity

Wheel Rail Contact Geometry

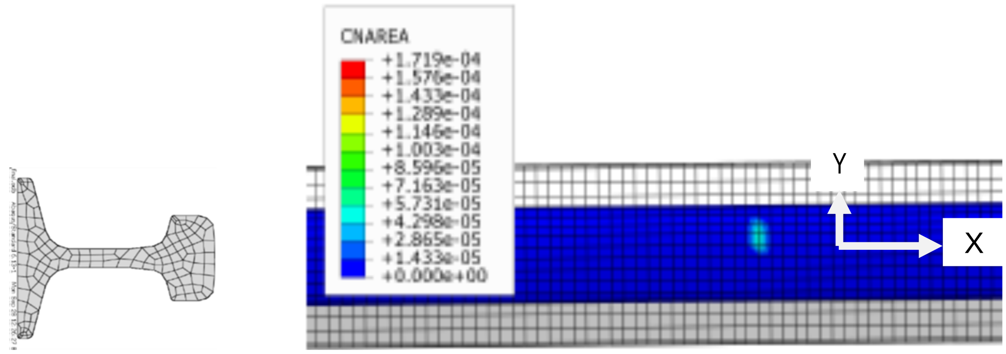

Figure A-5 Contact area geometry & location (30mm applied lateral irregularity for right rail)

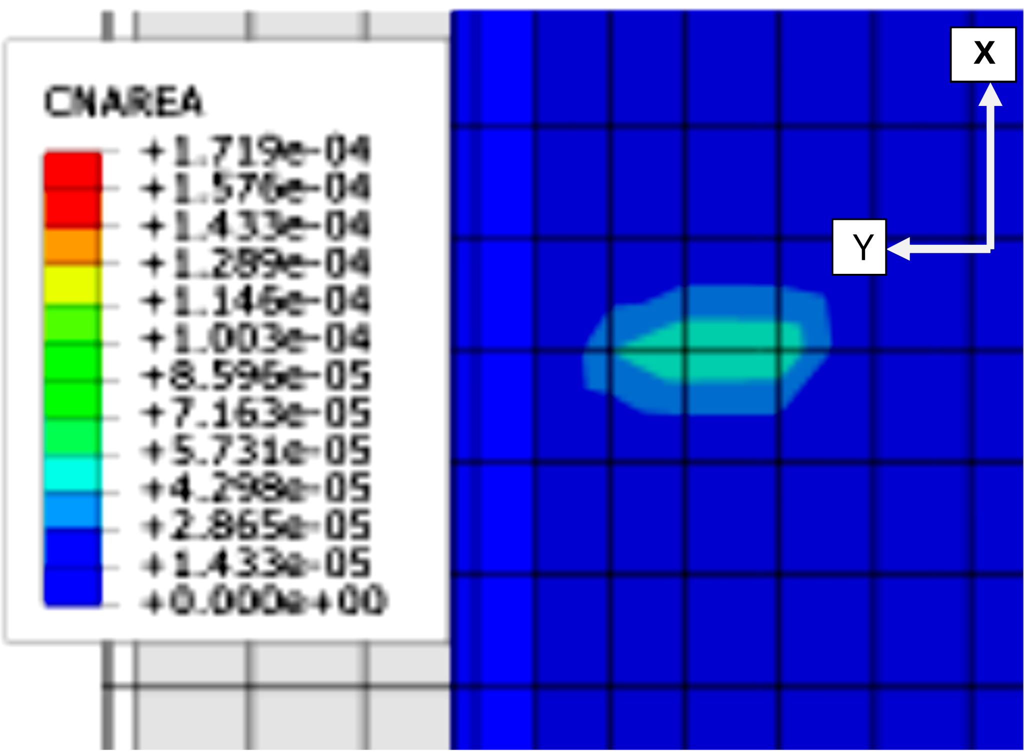

Figure A-6 Contact area contour- m^2 (30mm applied lateral irregularity for right rail)

Normal Contact pressure (30mm applied lateral irregularity for right rail)

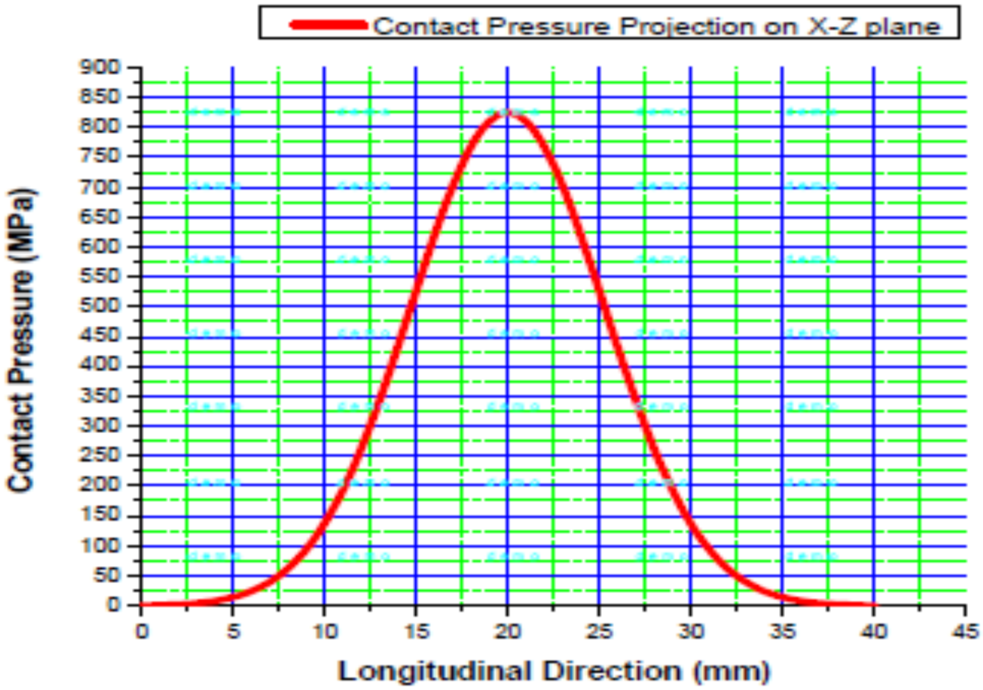

Figure A-7. Contact pressure projection on X-Z plane.

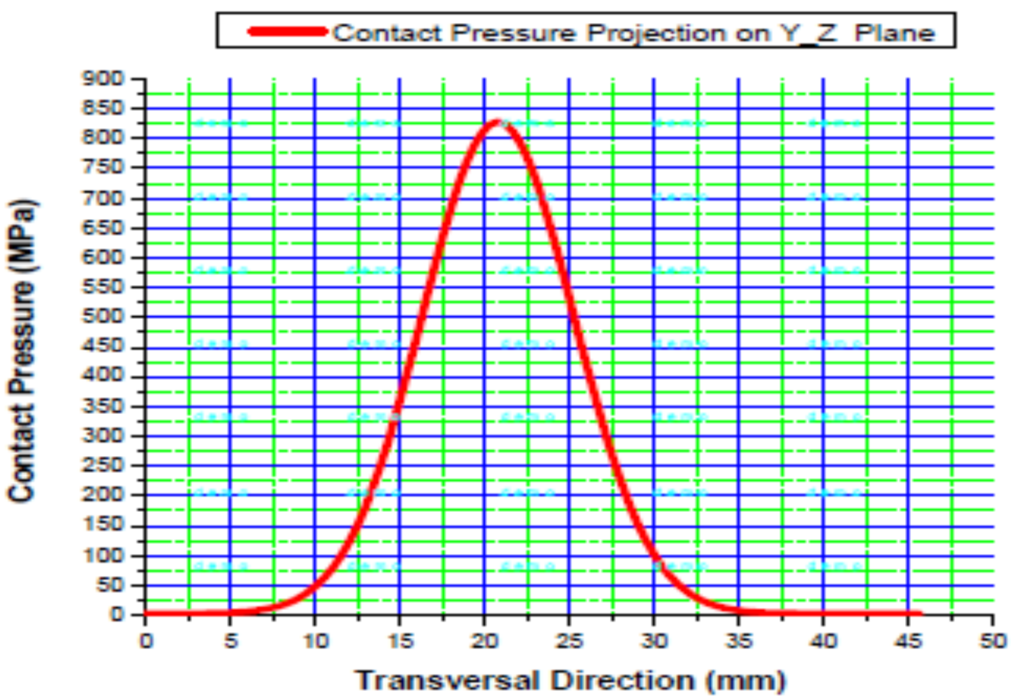

Figure A-8 Contact pressure projection on Y-Z plane.

Annex: B

Tracks with Longitudinal/Cross level irregularity

10mm Applied Irregularity

Wheel Rail Contact Geometry

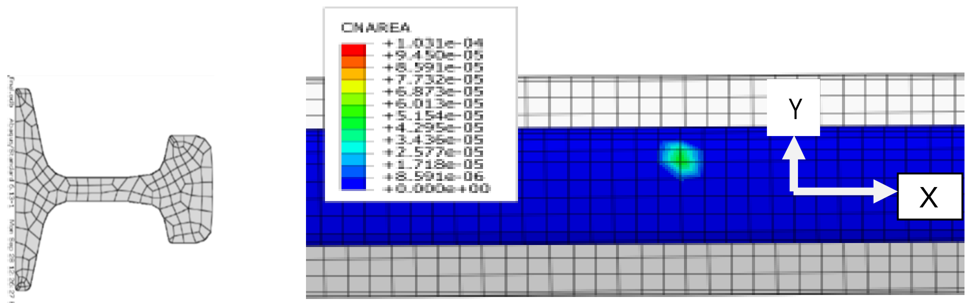

Figure B-1 Contact area geometry & location (10mm applied vertical irregularity for right rail)

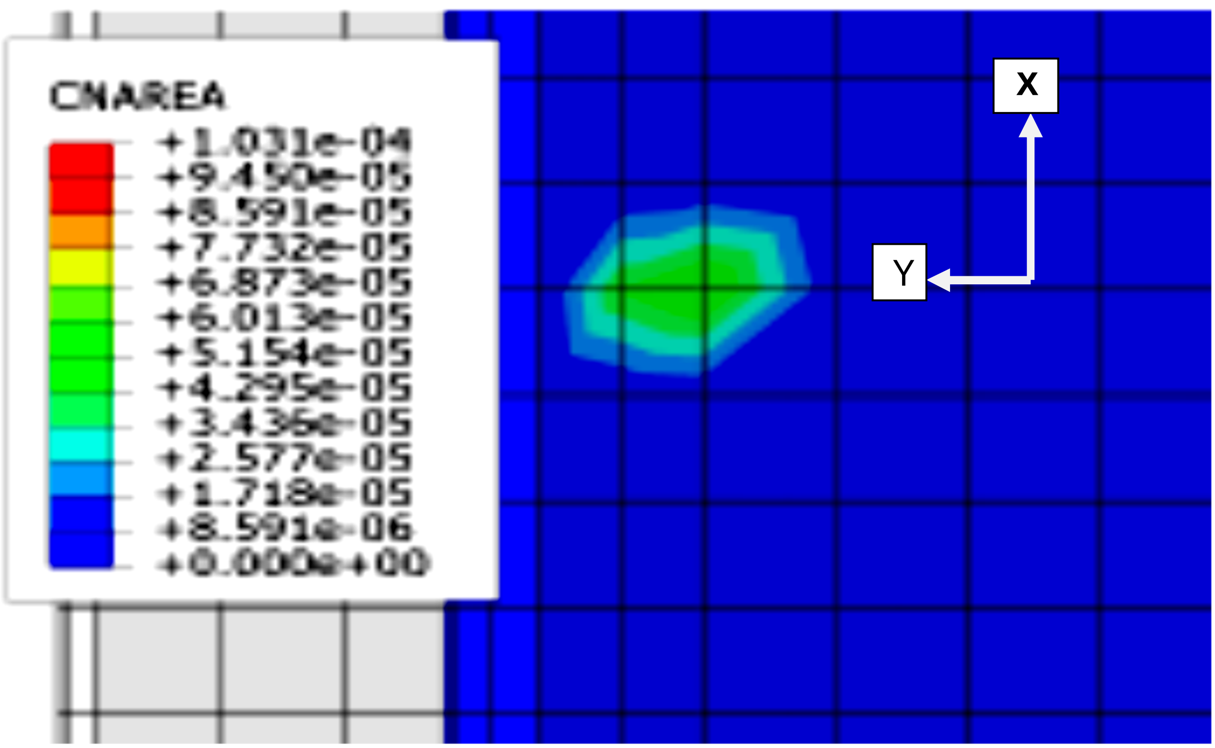

Figure B-2 Contact area contour -m^2- (10mm applied vertical irregularity for right rail)

Normal Contact pressure (10mm applied vertical irregularity for right rail)

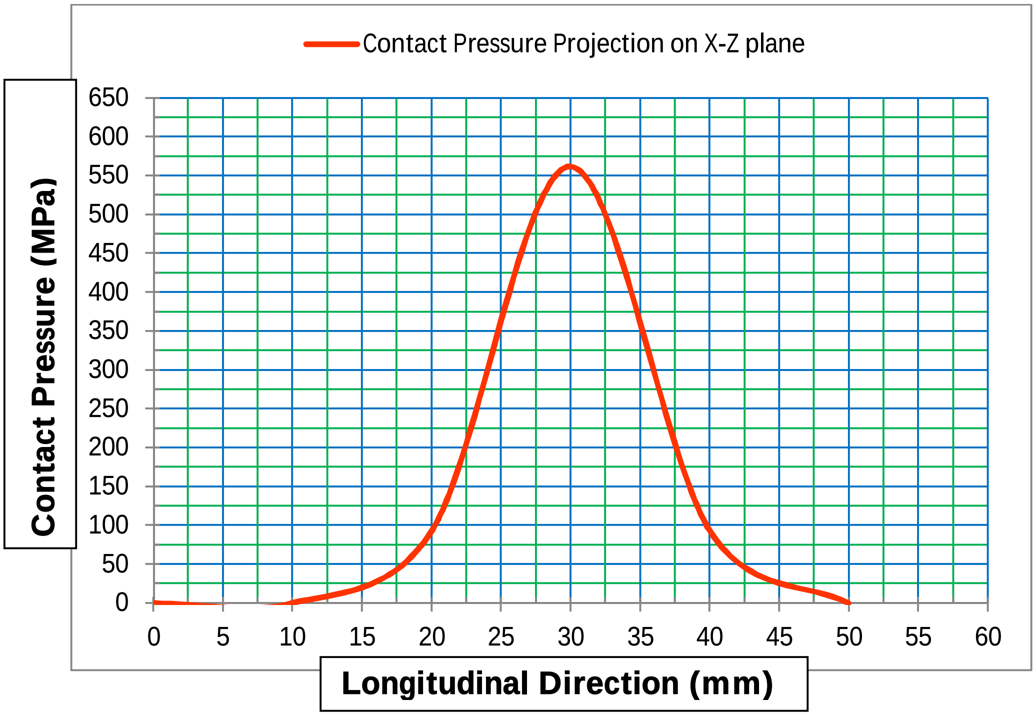

Figure B-3 Contact pressure projection on X-Z plane.

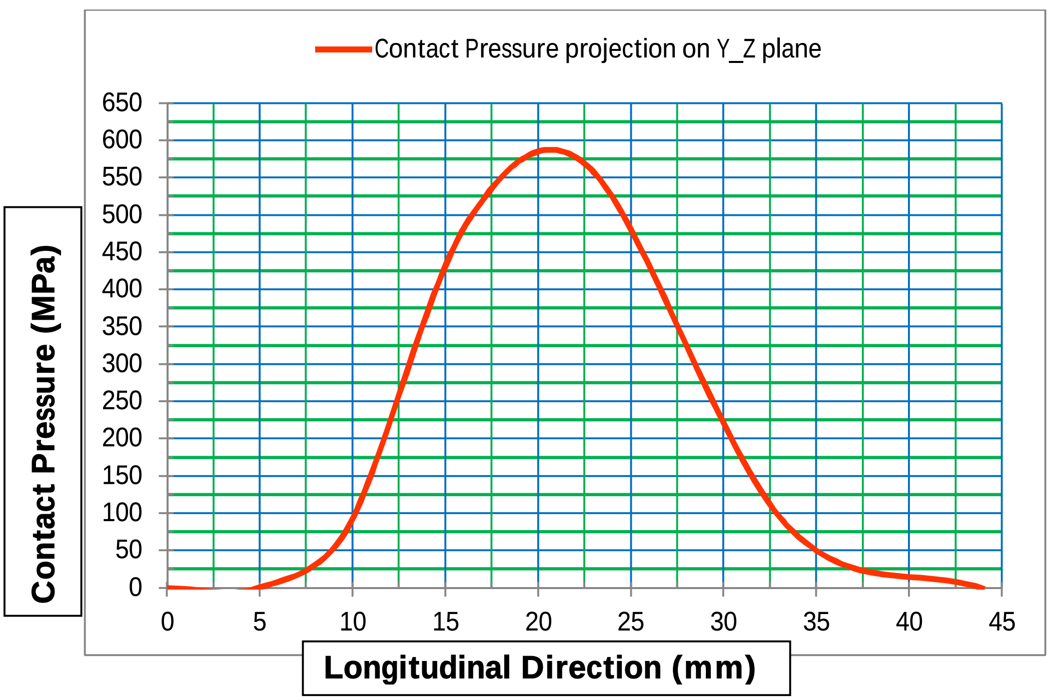

Figure B-4 Contact pressure projection on Y-Z plane.

30mm Applied Irregularity

Wheel Rail Contact Geometry

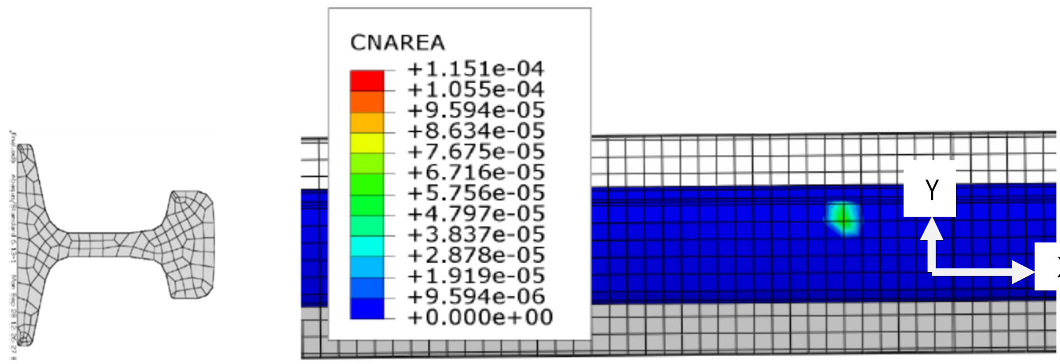

Figure B-5 Contact area geometry & location (30mm applied vertical irregularity for right rail)

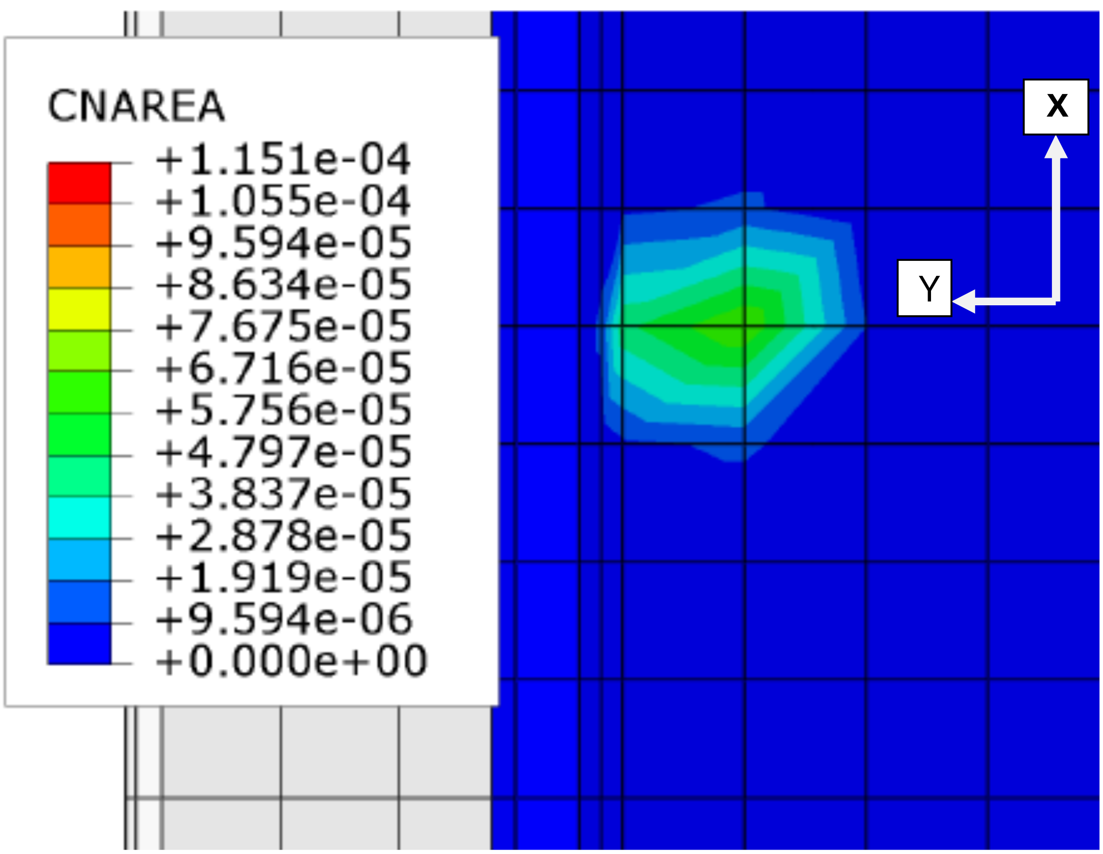

Figure B-6 Contact area contour -m^2- (30mm applied vertical irregularity for right rail)

Normal Contact pressure (30mm applied vertical irregularity for right rail)

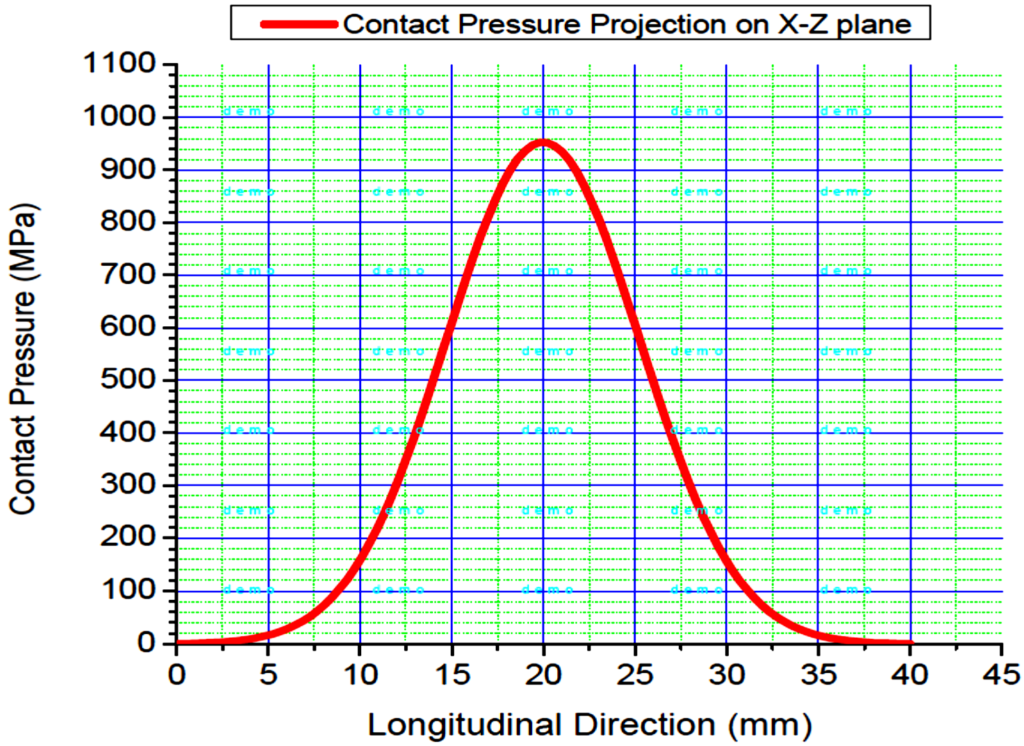

Figure B-7 Contact pressure projection on X-Z plane.

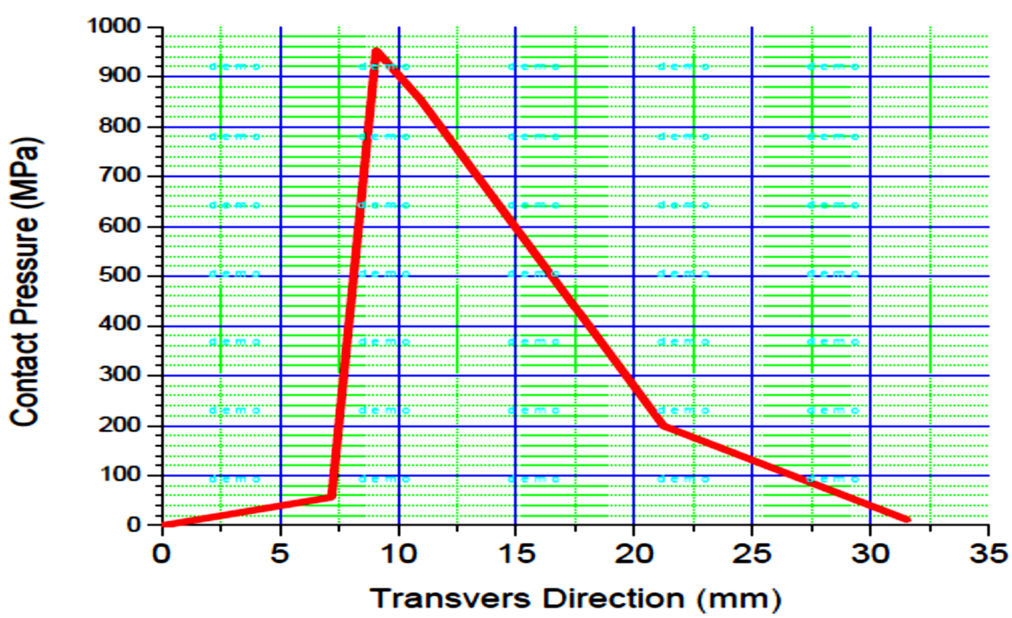

Figure B-8 Contact pressure projection on X-Z plane.